C.P. No. 119
(14,969)
A.R.C. Technical Report

MINISTRY OF SUPPLY

AERONAUTICAL RESEARCH COUNCIL
CURRENT PAPERS

Asymmetric Tailplane Loads Due to Sideslip

By

Winfried Braun

LONDON: HER MAJESTY'S STATIONERY OFFICE

1953

Price 8s. 6d. net

C.P. No.119

Technical Note No. Structures 81

January, 1952

ROYAL AIRCRAFT ESTABLISHMENT

Asymmetric Tailplane Loads Due to Sideslip

by

Winfried Braun

SUMMARY

A method is derived which estimates the tailplane rolling moment coefficient due to sideslip for use in strength calculations. The investigation covers the contributions to the rolling moment from the end-plate effect at the fin (twin fins are not considered), the dihedral of the tailplane, the effect of the body (which differs on the lee and windward-sides), the effects of sweep-back and plan form, and of unsymmetrical lift distribution on the main wing. An allowance is made for the influence of propeller slip-stream, and a tolerance suggested to cover inaccuracies of the method. Comparison with experiment shows good agreement. The method is summarised and an example given in appendices.

LIST OF CONTENTS

LIST OF APPENDICES

LIST OF ILLUSTRATIONS

LIST OF ILLUSTRATIONS (CONTD.)

NOTATION

A = Geometric aspect ratio

A_e = Effective aspect ratio

a = $\frac{dC_L}{d\alpha}$ = slope of the lift curve per radian angle of incidence

b = Span

b_{Vu} = Span of the fin and rudder above the tailplane

B = Breadth of the fuselage

$\bar{c}$ = Geometric mean chord

C_L = Lift coefficient

C_ℓ = $\frac{\text{Roll M}}{\frac{\rho}{2} V^2 Sb}$ = rolling moment coefficient

f_M = Glauert factor for correction of the lift curve slope due to Mach numbers

G = Factor which allows for aspect ratios differing from $A = 6$

H = Height of the fuselage

K = $\frac{dC_{\ell H}}{d\beta}$ = rolling moment derivative of the tailplane per radian angle of sideslip, positive if the windward side is turned down

ℓ_v = $\frac{dC_\ell}{d\beta}$ = rolling moment derivative per radian angle of sideslip

ℓ_{vp} = Rolling moment derivative per radian angle of sideslip due to plan form effect

M = Mach number

P_H = Load induced on one half of the tailplane

P_V = Load on the fin and rudder

Q = $\ell_v/(1 + \frac{B}{H})$ = Special value, giving the rolling moment due to fuselage effect

R = Correction factor for the end plate effect to allow for varying fore and aft horizontal position of the tailplane relative to the fin

S = Area

x = Position of the quarter-chord line of the tailplane behind the quarter-chord line of the fin and rudder

NOTATION (CONTD.)

z = Position of the wing or tailplane above or below the fuselage centre line

α = Angle of incidence, radian

β = Angle of sideslip, radian

Γ = Angle of dihedral, radian, positive tips up

Λ = Angle of sweep-back of the quarter-chord line, radian

τ = Taper ratio, tip chord divided by centre line chord

Suffices:-

H = Referring to the tailplane

V = " " " fin and rudder

Without suffix: referring to the main wing

1 Introduction

Unsymmetrical loads on the tailplane are critical for the design of the tailplane, since they affect the shear in the centre section, and apply torsion to the fuselage. In flight with sideslip, the magnitude of the stress depends on the rolling moment coefficient of the tailplane.

Thus, if the rolling moment is given by

$$\text{Roll M} = \tfrac{1}{2}\rho V^2 S_H b_H K \beta ,$$

where $K = \frac{dC_{\ell H}}{d\beta}$ is the rolling moment coefficient per radian angle of sideslip, the problem is solved as soon as K is known. The sign of K is positive for moments which turn the windward side of tailplane down.

The aim of this paper is to give a method for calculation of this coefficient with an accuracy sufficient for strength calculations. The method considers separately those effects which influence appreciably the rolling moment on the tailplane. The effects considered come from

(a) Lift on the fin, K_1,

(b) dihedral of the tailplane, K_2,

(c) fuselage influence on lee side, K_3,

(d) fuselage influence on windward side, K_4,

(e) dihedral of the main wing, K_5,

(f) fuselage influence on main wing, K_6,

(g) tailplane plan form and wing plan form, K_7,

(h) influence of propellers, K_8.

The total effect is considered to be the sum of all these particular effects. A small tolerance is added to cover inaccuracies of the method. The effect of Mach number is considered in an Appendix.

2 Rolling moment due to the lift on fin and rudder

One well known cause of tailplane rolling moment is due to the lift (lateral force) on the fin. The vortices produced by this lift (see Fig.1) change the angle of incidence of the tailplane and thus produce a rolling moment on the tailplane. It is greatest if the tailplane is at the upper or lower end of the fin, but of opposite sign, and it is zero if the tailplane is placed symmetrically in the centre of the fin.

A theoretical investigation of this effect by Rotta[2] was based on the assumption of a constant induced downwash at both fin and tailplane. This assumption has been proved invalid by Katzoff and Mutterperl[3] if the span of the tailplane is greater than that of the fin, as it is in most practical cases.

However, it is possible to modify this theory to obtain agreement with measurements by applying a correction factor; this has been done by Murray[4] and by Lyons and Bisgood[5]. Both papers correct the factor $\frac{A_e}{A}$ which is used to find the effective aspect ratio of the fin with consideration of the tailplane as an end plate.

The aspect ratio is increased because the development of the border vortices is hindered by the end plate and their induced downwash is therefore decreased. Since the induced rolling moment at the end plate is the reaction to this effect, it seems reasonable to apply the same correction, as for $\frac{A_e}{A}$, to the theoretical values of the rolling moment.

In Fig.2 the factor $\frac{A_e}{A}$ is plotted according to the theory corrected to agree with experiment. Using the effective aspect ratio A_e, the lift curve slope of the fin may be found from Fig.3.

Fig.4 shows the effect on the tailplane. The theoretical values of $\frac{P_H}{P_V}$ are plotted, i.e. the ratios between the load on one half of the tailplane and the load on the fin, corrected by the factor $(\frac{A_e}{A} - 1)$. The arm of the load may be assumed constant at $0.37 \frac{b_H}{2}$ for all practical ratios of $\frac{b_H}{b_V}$, in accordance with theory.

Another influence is provided by the horizontal position of the tailplane relative to the fin. It is possible to illustrate this effect using a simple model of the fin as a horseshoe vortex. When the tailplane is in the rearward position of Fig.6a the vortex has a greater influence than when the tailplane is in the forward position of Fig.6b.

Murray[4] measured the variation of the effective aspect ratio of a fin with the tailplane in various relative horizontal positions. He found that the increase in the effective aspect ratio is greater when the tailplane is in the rear-ward position and vice versa. The introduction of a factor R, based on measurements and plotted in Fig.5, can be used to include the effect of the relative fore and aft positions of the fin and the tailplane. The factor R multiplies the increase $(\frac{A_e}{A} - 1)$ given by Fig.2, and the same correction can therefore also be applied to the rolling moment on the tailplane, i.e. to P_H/P_V of Fig.4.

Further, we have to consider the ratio between the chords of the fin and rudder and the tailplane. The rolling moment will be smaller if the mean tailplane chord is smaller than the mean fin and rudder chord, and in the ratio of these chords. Thus we get

$$K_1 = 0.37 \; a_V \frac{S_V}{S_H} \frac{P_H}{P_V} \frac{\bar{c}_H}{\bar{c}_V} R$$

i.e.

$$K_1 = 0.37 \; a_V \frac{b_V}{b_H} \frac{P_H}{P_V} R \qquad (1)$$

The sign of K_1 is that of $\frac{P_H}{P_V}$, i.e. positive when the tailplane position is in the lower half of the fin, and negative if it is in the upper half. For span and area of the vertical plane we use the conventions suggested in Ref.5.

For comparison with experiment there is a reliable measurement of this contribution made on the "Hastings" aircraft. The rolling moment of the tailplane has been measured with and without fin. The experimental result was $\Delta K = 0.091$ for the addition of the fin, and calculation gives $\Delta K = 0.099$, which is fair agreement considering the roughness of the method and the experimental difficulties of measuring the effect. It should be stressed, however, that both the estimated and measured values do not include the changes caused by rudder deflection, and these may be considerable.

3 Rolling moment due to dihedral of the tailplane

To estimate the effect of the tailplane dihedral, Γ_H, we use the method given by Levacic[6]. When the angle of sideslip is β, there is a constant anti-symmetrical angle of incidence of $\beta\Gamma_H$ on both halves of the tailplane. We calculate the lift on each side, using a lift curve slope appropriate to half the geometric aspect ratio, and assume this lift acts at $\frac{4}{3\pi}$ of the semi-span. We then find:

$$K_2 = -0.212 \; a_{\left(\frac{A_H}{2}\right)} \Gamma_H \qquad (2)$$

where Γ_H is the dihedral angle of the tailplane in radians, positive when tip up, and $a_{\left(\frac{A_H}{2}\right)}$ the lift slope taken from Fig.3 for half the tailplane aspect ratio.

Measurements on the "Hastings" aircraft with various dihedral angles of the tailplane give the results below:

Tailplane dihedral.	Value of K	
	Fin present	Without fin
-10°	+0.103	+0.023
0	+0.034	-0.057
$+10^\circ$	-0.052	-0.143
$+15^\circ$	-0.098	-0.189

From these results we get an average value of $\Delta K = -0.48$ per radian dihedral, and our formula gives $\Delta K = -0.52$, which may be considered to be satisfactory agreement.

4 Rolling moment due to fuselage effect

(a) Lee side

It is evident that, when yawed, the fuselage will influence greatly the rolling moment on the tailplane. A theory has been developed[7] which gives the effect of the body on main wings in yaw. The fundamental idea is to split the velocity of the airstream round the fuselage into two components, one in the direction of the aircraft plane of symmetry (which gives no effect) and another perpendicular to this, i.e. in the direction of the span. The latter component has an inclination upwards or downwards and differs in front of the body and behind it (see Fig.7c). The rolling moment of the wing in this flow, per radian sideslip, can be evaluated; it is positive for low-wings, negative for high-wings, and zero for mid-wings. The results of this theory agree well with experiment, although the assumption, that the fuselage is of infinite length and of the same cross section as at the quarter chord line of the wing, is not true of actual aircraft.

The same method cannot be applied to the effect of the body on the tailplane. This may be explained by Fig.7a, where the streamlines on an aircraft are shown, when yawed through 10 degrees. Consider the streamlines which meet the tailplane on the lee side, most of them have crossed the fuselage at a section other than at the tailplane. Hence, if we want to apply the usual method, we should take body sections similar to those which the streamlines have passed. Thus for the lee side we consider the fuselage section at the wing (streamline II of Fig.7b). But the wing itself changes the flow around the fuselage at this section in such a way that the stagnation point is shifted to the root of the wing. The usual streamline pattern might therefore be applied here, if we replace the body section by an imaginary section consisting of the part of the body above the wing and its reflection at the wing root line (Fig.7c). The other streamlines (I and III of Fig.7b) traverse parts of the fuselage before or behind the wing and, if one wants to represent them by one streamline pattern only, it would be best to take the pattern for streamline II.

With this simplification we are now able to calculate the rolling moment using the work of Levacic[7] but extended to cover ratios of H/b appropriate to the tailplane. The resulting curves are presented in Fig.8. The value plotted is $Q = \dfrac{\ell_v}{1 + \frac{B}{H}}$ per radian yaw. The factor $(1 + \frac{B}{H})$ comes from theoretical considerations and allows for the slenderness of the body cross-section; $\frac{B}{H}$ is the ratio between body breadth and body height of the imaginary section. The curves are based on elliptical wings of aspect ratio $A = 6$, but we may apply them for other aspect ratios if we multiply them by the function $G(A)$ reproduced in Fig.9 from Ref.7.

There is a difficulty in deciding at which vertical position the tailplane should be placed relative to the body section at the wing (z of Fig.8), since, if the aircraft changes to a greater angle of incidence, the tailplane is at a lower position compared with the position when the wing is at zero-lift. However, from the strength aspect we are interested mainly in the high speed flight conditions when the fuselage axis lies approximately in the direction of the streamlines. It is sufficient, therefore, to consider this vertical position only.

Thus we ignore

(a) the effect of downwash on the streamlines,

(b) the fact that the fuselage cross section is generally less at the rear of the fuselage, and

(c) the fact that the simple approach gives a greater deviation of the stagnation point from the centre of the fuselage than occurs in practice. This results, with our method, in a fuselage of too great a height, except for mid-wings.

The neglect of (a) usually results in an under-estimate but this is probably balanced by the neglect of (b) and (c), both of which cause an over-estimate.

Thus we come to the following rule: Take the body section at the wing, but reflected at the wing root plane, and the position of the tailplane relative to this section when the fuselage axis is horizontal. If we then read off the value of Q from Fig.8 and $G_{(A_H)}$ from Fig.9 we get the rolling moment coefficient for the lee side as

$$K_3 = 0.5 \times Q \times \left(1 + \frac{B}{H}\right) \times G_{(A_H)} \tag{3}$$

The sign is positive if the tailplane position relative to the wing at the imaginary section is below and negative if it is above.

(b) <u>Windward Side</u>

As can be seen from Fig.7a, the streamlines passing the windward side of the tailplane have not crossed the fuselage at the wing and this side therefore must be treated differently to the leeward side. We consider that the body influences the tailplane in a similar manner to the wing; this will still be true if the tailplane is situated forward of the fin. The displacement of the flow by the fin is already considered in the end plate effect of the fin, but if there is a long dorsal fin this should be dealt with as if it belonged to the fuselage. Thus we take the body section at the leading edge of the tailplane and the vertical position of the tailplane relative to this section, and read off the appropriate value of Q from Fig.8. The rolling moment coefficient is then

$$K_4 = 0.5 \times Q \times \left(1 + \frac{B}{H}\right) \times G_{(A_H)} \tag{4}$$

In general, we get a large negative rolling moment from the lee side and the appropriate contribution from the windward side is small or even zero. The available measurements confirm these effects very clearly. Fig.10 shows the results of wind tunnel measurements on the Typhoon model[9]; of the rolling moment coefficient, which is negative in this case, roughly two thirds come from the lee side, and one third only from the windward side. Calculation, see Appendix 2 (or table I), gives K = -0.0835 for the lee side and K = -0.0306 for the windward side, and these agree well with the values measured.

Further confirmation comes from the flight measurements[10] shown in Fig.11. Calculation, without propeller influence, (see table I), gives K = -0.697 for the lee side and K = -0.0198 for the windward side. The experiments show that nearly the whole rolling moment comes from the lee side and a very small contribution only from the windward side, in good agreement with the calculation. We also see that this distribution does not depend much upon the propeller stream, for it is much the same with either port or starboard wing forward and with power off or on.

From the measurements on the Brabazon[11], shown in Fig.12, it can be seen that although the total rolling moment is positive the lee side again gives the more negative contribution. The values calculated without propeller stream are also plotted in the curves, but the agreement between calculation and measurement is not so close in this case as in others.

5 Effect of unsymmetrical lift distribution on the wing

(a) Dihedral of the main wing

An unsymmetrical lift distribution on the wing results in an unsymmetrical downwash which produces a rolling moment at the tailplane. This tailplane rolling moment is opposite in sign to that on the wing.

We may approach the calculation of this effect by using the known fact that the downwash angle at the tailplane is usually about half the angle of incidence at the main wing. This is true for symmetrical angles of incidence over the whole wing only, but it will be a reasonable first approximation for anti-symmetrical angles too. However, for an anti-symmetrical distribution on the wing the mutual interference between the downwash from one side and the upwash from the other will cause some reduction in the effective downwash at the tailplane. To allow for this, we shall take a quarter instead of half the angle of incidence at the wing.

Now, if the rolling moment coefficient at the wing is $\left(\frac{dC_\ell}{d\beta}\right)_W$ per radian angle of yaw, and if this is caused by an anti-symmetrical angle of incidence $\pm\,\Delta\alpha$, which is constant on each side, and positive on the windward side, we may calculate the rolling moment using strip theory, assuming the lift curve slope, a, appropriate to half the wing aspect ratio, and taking the lift as acting at $\frac{4}{3\pi}$ of the semi-span. Hence

$$\left(\frac{dC_\ell}{d\beta}\right)_W = -a_{\left(\frac{A}{2}\right)} \cdot |\Delta\alpha| \cdot \frac{2}{3\pi} .$$

In the same way we get for an anti-symmetrical angle $\Delta\alpha_H$ at the tailplane

$$K = -a_{\left(\frac{A_H}{2}\right)} \cdot |\Delta\alpha_H| \cdot \frac{2}{3\pi} \tag{5a}$$

If we calculate $\Delta\alpha$ from the first equation and put $\Delta\alpha_H = -\frac{1}{4}\,\Delta\alpha$, we get

$$K = -\frac{1}{4}\,\frac{a_{\left(\frac{A_H}{2}\right)}}{a_{\left(\frac{A}{2}\right)}} \times \left(\frac{dC_\ell}{d\beta}\right)_W \tag{5b}$$

This equation may be used when $\left(\frac{dC_\ell}{d\beta}\right)_{Wing}$ is known.

If $\left(\frac{dC_\ell}{d\beta}\right)_{Wing}$ is not known, but the dihedral angle of the wing is Γ radians, then for an angle of yaw of β radians, $\Delta\alpha = \beta\Gamma$, i.e.

$$\Delta\alpha_H = -\tfrac{1}{4}\beta\Gamma$$

and directly from equation 5a we get

$$K = a_{\left(\frac{A_H}{2}\right)} \frac{\Gamma}{4} \frac{2}{3\pi}$$

$$K_5 = 0.053 \quad a_{\left(\frac{A_H}{2}\right)}\Gamma \qquad (6)$$

(b) Influence of the fuselage on the main wing

The rolling moment on the main wing caused by the influence of the body has to be dealt with a little differently. As before, we take $\Delta\alpha_H = -\frac{1}{4}\Delta\alpha$. In this case, the anti-symmetrical angle of incidence of the wing is not constant along each semi-span, but is greatest close to the fuselage and decreases rapidly at the wing tips.

However, if we assume the distribution of this angle of incidence to be the same at the tailplane as at the wing, but a quarter the magnitude and of opposite sign, we may use the values of $Q = \dfrac{\ell_v}{1 + \frac{B}{H}}$ as given in Fig. 8, and apply this result to the tailplane with the smaller span. If we assume a ratio of $\frac{b_H}{b} = \frac{1}{3}$, which is an average value for practical aircraft, we find that for the fuselage widths of typical aircraft we get a reasonably constant ratio between Q for the tailplane and Q for the wing which is

$$\frac{Q_H}{Q_{Wing}} \sim 6.0$$

To correct for the aspect ratio of the tailplane we have to multiply by the appropriate factor $G_{(A_H)}$ from Fig. 9.

Thus we get

$$K = -6 \times \tfrac{1}{4}\, Q \times \left(1 + \tfrac{B}{H}\right) \times G_{(A_H)}$$

$$K_6 = -1.5 \times Q \times \left(1 + \tfrac{B}{H}\right) \times G_{(A_H)} \qquad (7)$$

where Q and $\frac{B}{H}$ apply to the sections at the wing.

6 Effects depending on lift

(a) Effects of the tailplane and the wing plan forms

The effects dealt with so far can be regarded as independant of the lift. There are other effects, however, which depend only upon the lift. The first of these is the influence of the tailplane plan form, and we shall consider now this effect for a straight wing, and later superimpose the effect of sweep.

An untwisted wing with no lift produces no rolling moment in sideslip, but if it has an angle of incidence, i.e. lift, a rolling moment is produced. When the wing is yawed the lift distribution is changed by three effects: 1. by the oblique location of the vortex sheet, 2. by the lateral flow along the wing span and 3. by the alteration of the incident velocity ($V \cos \beta$ instead of V). The first two effects produce a rolling moment, the magnitude of which depends on the wing plan form and aspect ratio. Theoretical calculations by Weissinger[12,13] are in good agreement with available measurements[7] and can therefore be used as a basis. They are represented in Fig.13, and the value $\frac{\ell_{vp}}{C_L}$ per radian angle of sideslip has been plotted for various aspect ratios and taper ratios, and for elliptical wings. Reading off this value for the parameters appropriate to the tailplane, we obtain

$$K = \left(\frac{\ell_{vp}}{C_L}\right)_H C_{L_H} \tag{8}$$

where C_{L_H} is the lift coefficient of the tailplane, whether produced by incidence or elevator deflection. We see, from Fig.13, that the effect is considerable only for small aspect ratios and plan forms close to the rectangular one.

We may also consider the same effect at the main wing, which, by means of the downwash, gives a rolling moment of opposite sign at the tailplane. We have already derived the general formula (5b). If we put

$$\left(\frac{dC_\ell}{d\beta}\right)_W = \left(\frac{\ell_{vp}}{C_L}\right)_{Wing} \cdot C_L \quad \text{we get}$$

$$K = -0.25 \frac{a\left(\frac{A_H}{2}\right)}{a\left(\frac{A}{2}\right)} \left(\frac{\ell_{vp}}{C_L}\right)_{Wing} C_L \tag{9}$$

(b) Effect of sweep-back of the tailplane and of the wing

For a swept wing in yaw, an anti-symmetric angle of attack occurs on the halves of the wing. The resulting rolling moment has been calculated[7] and is given by

$$\frac{\ell_{vSweep}}{C_L} = -0.268 \sin\Lambda \quad \text{per radian yaw,}$$

for an elliptical wing of aspect ratio $A = 6$, Λ being the angle of sweep-back of the quarter chord line. For other aspect ratios we multiply this value by the function $G_{(A)}$ given in Fig.9. We therefore get for a tailplane with sweep-back Λ_H

$$K = -0.268 \sin \Lambda_H \cdot C_{L_H} \cdot G(A_H) \tag{10}$$

In the same way, we may calculate the rolling moment due to the sweep-back of the wing, and estimate the reaction at the tailplane using equation (5b). Thus

$$\left(\frac{dC_\ell}{d\beta}\right)_W = -0.268 \sin \Lambda \cdot G_{(A)} \cdot C_L$$

whence

$$K = 0.067 \sin \Lambda \cdot \frac{a\left(\frac{A_H}{2}\right)}{a\left(\frac{A}{2}\right)} \cdot G_{(A)} \cdot C_L \tag{11}$$

where C_L is the lift coefficient of the wing.

The total dependance on C_L and C_{L_H} therefore, from equations (8), (9), (10) and (11), is

$$K_7 = \frac{a\left(\frac{A_H}{2}\right)}{a\left(\frac{A}{2}\right)} \left\{-0.25 \left(\frac{\ell_{vo}}{C_L}\right)_W + 0.067 \cdot G_{(A)} \cdot \sin \Lambda\right\} C_L +$$

$$\left\{\left(\frac{\ell_{vp}}{C_L}\right)_H - 0.268 \cdot G_{(A_H)} \cdot \sin \Lambda_H\right\} C_{L_H} \tag{12}$$

7 Effect of propellers

The slipstream from propellers affects the rolling moment on the tailplane. Even when the aircraft is not yawed there may be some rotation of the slipstream, and when the aircraft is yawed there will be changes in the wake pattern from the propeller. A method which took into account the many possible propeller variations would be very complex indeed. Thus we will confine ourselves to a somewhat arbitrary procedure based on the measurements shown in Figs.10 and 11.

The most critical conditions of tailplane loading arise in sideslip. It seems reasonable, therefore, to consider the propeller contribution to the tailplane rolling moment when the aircraft is yawed through $\pm 10^\circ$ and to translate this in terms of K to conform with the treatment adopted for the other effects. In this way a value of

$$K_8 = \pm 0.015 \tag{13}$$

is suggested as generally sufficient to allow for the effect of the propeller slipstream.

8 Limits of accuracy

We cannot expect great accuracy, in view of the rather rough assumptions. Moreover, there are other minor influences which have not been considered and which may produce a rolling moment, for example slight differences in the airplane on the two sides of the plane of symmetry (see Ref.14). For these reasons it is advisable to include a tolerance in any estimate of K. A tolerance of

$$\Delta K = \pm 0.025 \tag{14}$$

seems reasonable and sufficient to cover all possible errors.

This method does not include the effect of high Mach numbers, but, as shown in Appendix 3, it is possible to include this effect by multiplying those contributions independent of C_L (i.e. K_1 to K_6) by a factor

$$f_M\left(\frac{A_H}{2}\right) = \frac{1 + \frac{4}{A_H}}{\sqrt{1 - M^2} + \frac{4}{A_H}} \tag{15}$$

9 Comparison with measurements

Table I compares the rolling moment coefficients estimated by the method proposed with those measured in the wind tunnel or in flight. The separate contributions are given. In Appendix II the calculations for an aircraft are given in detail. The contributions depending on lift are not included in these examples, since they are small, and no contributions were added for propeller effects, because the experimental values are either without propeller or the average between power off and on. Fig.14 shows the side-views of the aircraft examined.

The experimental results sometimes show a considerable scatter (see Table II) if some parameters are varied, such as the angle of incidence of the aircraft or the tailplane, elevator deflection, propeller thrust, and magnitude or direction of the angle of yaw. In such cases an average value is used for comparison.

Table I indicates, that the method proposed gives the correct sign and the right order of magnitude, and that inclusion of the suggested tolerance of $\Delta K = \pm 0.025$ covers all the measured values.

10 Conclusions

The method proposed gives results which are in satisfactory agreement with measurements. It might therefore be used for the calculation of the unsymmetrical loads on tailplanes in those cases where no reliable wind tunnel measurements are available.

REFERENCES

No.	Author	Title, etc.
1	-	Design Requirements for Aeroplanes, A.P.970, including amendment list 48.
2	Rotta, J.	Luftkräfte am Tragflügel mit einer seitlichen Scheibe. Ing. Archiv, Vol. XIII, 1942, page 119-131.
3	Katzoff, S. and Mutterperl, W	The end plate effect of a horizontal tail surface on a vertical tail surface. N.A.C.A. Tech. Note No.797, 1941.
4	Murray, H.E.	Wind tunnel investigation of end-plate effects on horizontal tails on a vertical tail compared with available theory. N.A.C.A. Tech. Note No. 1050, 1946
5	Lyons, D.J. and Bisgood, P.L.	An analysis of the lift slope of aerofoils of small aspect ratio, including fins, with design charts for aerofoils and control surfaces. R. & M. 2308, 1950.
6	Levacic, I.	Rolling moment due to sideslip. Part I. The effect of dihedral R.A.E. Report No. Aero 2028, 1945.
7	"	Part II. The effect of sweep-back and plan form. ARC.9278.
8	"	Part IIIA. The effect of wing body arrangement. ARC.9987.
9	Hills, R. and Warren, C.H.E.	Wind tunnel tests on the Typhoon to determine the loads on the tail and fin. ARC.7789.
10	Sadoff, M. and Clowning, A.C.	Measurements of the pressure distribution on the horizontal tail surface of a typical propeller-driven pursuit airplane in flight. II. The effect of angle of sideslip and propeller operation. N.A.C.A. Tech. Note No. 1202, 1947.
11	Bristol Aeroplane Co. Ltd.	Bending moment tests on tailplane due to sideslip. Bristol Report No. F.N.105, 1945.
12	Weissinger	Der schiebende Tragflügel bei gesunder Strömung. Lilienthal Gesellschaft für Luftfahrtforschung, Bericht S.2, 1938-39.
13	Weissinger	Ergänzungen und Berichtigungen zur Theorie des schiebenden Flügels. Vorabdrucke aus Jahrbuch 1943 der deutchen Luftfahrtforschung, Band 10 (1943), Heft 7.
14	Sweborg, H.H. and Dingeldein, R.C.	Effects of propeller operation and angle of yaw on the distribution of the load on the horizontal tail surface of a typical pursuit airplane. N.A.C.A. ARR. No.4B10, 1944.

APPENDIX I

Summary of the method

First collect the basic data. These are:-

Wing:

b = ft

S = sq.ft

A =

$\frac{A}{2}$ =

Γ = radian

Λ = radian

τ =

Horizontal tailplane, including elevator:

b_H = ft

S_H = sq.ft

A_H =

$\frac{A_H}{2}$ =

Γ_H = radian

Λ_H = radian

τ_H =

Vertical tailplane, including rudder:

b_V = ft (as defined in (5) i.e. including the fuselage width below the centre of fin and rudder).

S_V = sq.ft (including the fuselage below the fin, but only up to the defined span, compare Fig.15b).

A_V =

Λ_V = radian

$\bar{c}_V$ = ft

1 End plate effect

We consider a cross section at the tailplane, see Fig.15a, and read off $\frac{b_{VU}}{b_V}$ and $\frac{b_H}{b_V}$. From Fig.2, we take $\frac{A_e}{A}$ corresponding to these parameters, and find the effective aspect ratio of the fin $A_e = \frac{A_e}{A} \times A_V$.

With this value A_e we find a_V from Fig.3. It is not advisable to use a correction if the fin is swept, because this effect is negligible for the generally small aspect ratios of the fin. Next we read off the value $\frac{P_H}{P_V}$ from Fig.4 for the parameters $\frac{b_{VU}}{b_V}$ and $\frac{b_H}{b_V}$. Next we consider a side view of the fin with the tailplane (see Fig.15b) and estimate the average position of the quarter-chord line of the fin and the quarter-chord line of the tailplane; sweep-back should be considered here. We read off the distance x (ft), i.e. the position of the quarter-chord line of the tailplane behind or before the quarter-chord line of the fin and rudder; x is positive for a rearward position of the tailplane. We calculate $\frac{x}{c_V}$, and take the value for the correction factor R from Fig.5.

We now introduce all values in formula (1)

$$K_1 = 0.37 \; a_V \frac{b_V}{b_H} \frac{P_H}{P_V} R \qquad (1)$$

2 Dihedral of the tailplane

We read off the value of the lift curve slope $a\left(\frac{A_H}{2}\right)$ for the aspect ratio $\frac{A_H}{2}$, using Fig.3. When $\frac{A_H}{2} \leq 1.5$ no correction factor to "a" should be applied for sweep of the tailplane, but for $\frac{A_H}{2} > 1.5$ it should be multiplied by a factor $\frac{1 + \cos \Lambda_H}{2}$. We introduce the values into formula (2)

$$K_2 = -0.212 \; a_{\left(\frac{A_H}{2}\right)} \; \Gamma_H \qquad (2)$$

3 Fuselage influence on lee side

We consider a cross section through the fuselage at the quarter-chord position of the main wing, (Fig.15c) and mark the position of the tailplane relative to this cross section when the air stream is parallel to the fuselage axis. We now replace this section by one which is given if that part of the body on the same side of the wing as the tailplane is reflected at the main wing (See Fig.15d). We read off the height H of this imaginary fuselage, its breadth B, and the distance z of the tailplane from the horizontal axis of symmetry, calculate the values $\frac{H}{b_H}$ and $\frac{z}{H}$, and read off the value Q from Fig.8. Q is positive if the position of the tailplane is below the wing, negative if it is above. We further take the correction factor G from Fig.9 for the tailplane aspect ratio A_H. We now introduce all values into formula (3)

$$K_3 = 0.5 \times Q \times \left(1 + \frac{B}{H}\right) \times G_{(A_H)} \qquad (3)$$

4 Fuselage influence on windward side

We consider a cross section through the fuselage at the leading edge of the horizontal tailplane (Fig.15d). If there is a long dorsal fin which was not included in the fin area, we have to allow for this by considering it as belonging to the fuselage. Calculate $\frac{H}{b}$ and $\frac{z}{H}$ and read off Q from Fig.8. We then find

$$K_4 = 0.5 \times Q \times \left(1 + \frac{B}{H}\right) \times G_{(A_H)} \qquad (4)$$

5 Dihedral of the main wing

Using the same value for $a_{\left(\frac{A_H}{2}\right)}$ as in para.2, we find with equation (6)

$$K_5 = 0.053 \; a_{\left(\frac{A_H}{2}\right)} \cdot \Gamma \qquad (6)$$

6 Fuselage influence on main wing

We consider a cross section through the body at the wing, which is the same as first used in para.3, (Fig.15c) but without the tailplane, and read off $\frac{H}{b}$ and $\frac{z}{H}$ for the position of the wing. Fig.8 gives us Q, and we find K from formula (7)

$$K6 = -1.5 \times Q \times \left(1 + \frac{B}{H}\right) \times G_{(A_H)} \qquad (7)$$

7 Effects depending on C_L and C_{LH}

For the aspect ratio of the wing and taper-ratio of the wing, we read off from Fig.13 the value of $\left(\frac{\ell_{vp}}{C_L}\right)_{Wing}$, and, in the same way for the appropriate parameters of the tailplane, the value $\left(\frac{\ell_{vp}}{C_L}\right)_H$. Furthermore Fig.3 gives $a_{\left(\frac{A_H}{2}\right)}$ and $a_{\left(\frac{A}{2}\right)}$, and Fig.9 $G_{(A)}$ and $G_{(A_H)}$. We introduce these values into equation (12)

$$K_7 = \frac{a_{\left(\frac{A_H}{2}\right)}}{a_{\left(\frac{A}{2}\right)}} \left\{-0.25 \left(\frac{\ell_{vp}}{C_L}\right)_W + 0.067 \; G_{(A)} \sin \Lambda \right\} C_L +$$

$$\left\{\left(\frac{\ell_{vp}}{C_L}\right)_H - 0.268 \cdot G_{(A_H)} \sin \Lambda_H \right\} C_{L_H} \qquad (12)$$

where Λ and Λ_H are the angles of sweepback of the quarter-chord line of the wing and the tailplane.

8 Propeller influence

To allow for the propeller influence we take

$$K_8 = \pm 0.015 \tag{13}$$

9 Tolerances

To include tolerances, we add

$$\Delta K = \pm 0.025 \tag{14}$$

10 Total Value

The total value is given by

$$K = K_1 + K_2 + K_3 + K_4 + K_5 + K_6 + K_7 + K_8 + \Delta K$$

11 Mach number effect

If we have to consider the effect of Mach number, then for Mach numbers up to 0.8 we calculate according to equation (15)

$$f_{M\left(\frac{A_H}{2}\right)} = \frac{1 + \frac{4}{A_H}}{\sqrt{1 - M^2} + \frac{4}{A_H}} \tag{15}$$

and get, with Mach number effect,

$$K = (K_1 + K_2 + K_3 + K_4 + K_5 + K_6)\, f_{M\left(\frac{A_H}{2}\right)} + K_7 + K_8 + \Delta K$$

For Mach numbers greater than 0.8 the same value as for M = 0.8 should be taken in lieu of better data.

APPENDIX II

Example

The calculation may be shown in detail for the example of the Typhoon.

We collect the fundamental data

Wing:

$b \;=\; 41.6$ ft

$S \;=\; 279$ sq.ft

$A \;=\; 6.20$

$\frac{A}{2} \;=\; 3.10$

$\Gamma \;=\; 4.5^{\circ}$ (average) $=\; 0.0785$ rad.

$\Lambda \;=\; 0^{\circ}$

$\tau \;=\; 0.50$

Horizontal tailplane:

$b_H \;=\; 13.0$ ft

$S_H \;=\; 43.9$ sq.ft

$A_H \;=\; 3.86$

$\frac{A_H}{2} \;=\; 1.93$

$\Gamma_H \;=\; 0^{\circ}$

$\Lambda_H \;=\; 0^{\circ}$

$\tau_H \;=\; 0.61$

Vertical tailplane:

$b_V \;=\; 6.5$ ft

$S_V \;=\; 33.3$ sq.ft

$A_V \;=\; 1.27$ (geometric)

$\Lambda_V \;=\;$ assumed 0

$\bar{c}_V \;=\; 5.12$ ft

1 End plate effect

The dimensions of the cross section at the tailplane are given in Fig.15a, and we find:

$$\frac{b_{VU}}{b_V} = 0.626 \quad ; \quad \frac{b_H}{b_V} = 2.00$$

From Fig.2 we find $\frac{A_e}{A}$ = 1.02 so that A_{eff} = 1.02 × 1.27 = 1.30, and from Fig.3 we get a_V = 1.77.

From Fig.4 we read off $\frac{P_H}{P_V}$ = + 0.09.

From the sketch Fig.15b we find x = -1.8 ft, and thus $x/\bar{c}_V$ = -0.351.

The value R = 0.65 is given by Fig.5.

Thus from equation (1)

$$K_1 = 0.37 \times 1.77 \times \frac{6.5}{13} \times 0.09 \times 0.65$$

$$K_1 = 0.0192$$

2 Dihedral of the tailplane

Since there is no dihedral, we find K_2 = 0.

3 Fuselage influence on lee-side

Fig.15c gives the cross section at the wing with the position of the tailplane for the fuselage axis parallel to the flow. Fig.15d gives the imaginary cross section, if the fuselage is reflected at the wing. We read off

$$\frac{H}{b_H} = \frac{7.8}{13} = 0.600 \quad ; \quad \frac{z}{H} = \frac{2.52}{7.8} = 0.323$$

and this gives from Fig.8 a value Q = -0.1323.

From Fig.9 we find $G_{(A_H)}$ = 0.83. We now introduce into equation (3) and

$$K_3 = -0.5 \times 0.1323 \left(1 + \frac{3.55}{7.8}\right) \times 0.83$$

$$K_3 = -0.0798$$

4 Fuselage influence on windward side

The cross section through the fuselage at the leading edge of the horizontal tailplane is given in Fig.15e, and we find

$$\frac{H}{b_H} = \frac{3.2}{13} = 0.246 \quad ; \quad \frac{z}{H} = \frac{0.8}{3.2} = 0.25,$$

which gives, from Fig.8, $Q = -0.042$. $G_{(A_H)} = 0.83$ is the same as before, and from equation 4 we find

$$K_4 = -0.5 \times 0.042 \times \left(1 + \frac{1.75}{3.2}\right) \times 0.83$$

$$K_4 = -0.0270$$

5 Dihedral of the main wing

For half the aspect ratio of the tailplane $\frac{A_H}{2} = 1.93$ we find from Fig.3 $a_{\left(\frac{A_H}{2}\right)} = 2.40$, and with equation (6)

$$K_5 = 0.053 \times 2.40 \times 0.0785$$

$$K_5 = 0.0100$$

6 Fuselage influence on the main wing

The cross section through the body at the main wing is the same as in Fig.15c (but without the tailplane plotted there). We find

$$\frac{H}{b} = \frac{5}{41.6} = 0.12 \quad ; \quad \frac{z}{H} = \frac{2}{5} = 0.40,$$

and Fig.8 gives $Q = 0.0172$. $G_{(A_H)} = 0.83$ is the same again, so that equation (7) gives

$$K_6 = -1.5 \times 0.0172 \times \left(1 + \frac{3.55}{5}\right) \times 0.83$$

$$K_6 = -0.0365$$

7 Effects depending on C_L and C_{L_H}

For the aspect ratio of the wing $A = 6.20$ and taper ratio of the wing $\tau = 0.5$ we find from Fig.13

$$\left(\frac{\ell vp}{C_L}\right)_W = -0.011,$$

and for the tailplane with $A_H = 3.86$ and $\tau_H = 0.61$ we find

$$\left(\frac{\ell v_D}{C_L}\right)_H = -0.057$$

Fig.3 gives $a_{\left(\frac{A_H}{2}\right)} = 2.40$ and $a_{\left(\frac{A}{2}\right)} = 3.15$

Since $\Lambda = \Lambda_H = 0$, we find from equation (12)

$$K_7 = 0.25 \times \frac{2.40}{3.15} \times 0.011 \times C_L - 0.057 \times C_{L_H}$$

$$K_7 = 0.0021 \times C_L - 0.057 \times C_{L_H}$$

8 Effect of propellers

According to equation (13) $K_8 = \pm 0.015$.

9 Tolerances

We add

$$\Delta K = \pm 0.025$$

10 Total value

Adding all contributions, we find the total value

$$K = -0.1141 + 0.0021\, C_L - 0.057 \times C_{L_H} \pm 0.040$$

Since the contributions depending on C_L and C_{L_H} are small, for the high speed flight conditions which give the greatest loads on the tailplane, we may neglect them and have

$$K = -0.114 \pm 0.040.$$

APPENDIX III

The effect of High Mach numbers

It is possible to extend our theory for higher Mach numbers within the range of validity of Glauert's rule. Since the changes of angles of incidence considered in the theory are generally rather small, one could assume Glauert's rule to be valid up to about $M = 0.8$. Thus we should multiply the lift curve slope by the corresponding Glauert factor for the appropriate aspect ratio. This factor is

$$f_{M(A)} = \frac{1 + \frac{2}{A}}{\sqrt{1 - M^2} + \frac{2}{A}} \qquad (16)$$

Let us now consider how each of the effects discussed changes with the Mach number.

1. End plate effect, formula (1)

The factor a_V increases with $f_{M(A_V)}$. The ratio $\frac{P_H}{P_V}$ may be written as $\frac{\alpha_H \times a_{\left(\frac{A_H}{2}\right)}}{\beta_V \times a_{(A_V)}}$. If we consider that the effect is caused by changes of the angle of incidence at the tailplane, and these changes remain proportional to the changes of the angles of incidence at the fin, $\frac{P_H}{P_V}$ increases with a factor $\frac{f_{M\left(\frac{A_H}{2}\right)}}{f_{M(A_V)}}$.

X This assumption leaves out the increase in the lift curve slope of the fin.

The total effect therefore increases with $f_{M\left(\frac{A_H}{2}\right)}$.

2. Dihedral of the tailplane, formula (2)

The effect increases with $f_{M\left(\frac{A_H}{2}\right)}$

3. Fuselage effect on the lee-side, formula (3)

If we assume the streamline pattern to be the same as at low Mach numbers, the angles of incidence are unchanged and the rolling moment increases as $a_{\left(\frac{A_H}{2}\right)}$ i.e. as $f_{M\left(\frac{A_H}{2}\right)}$

4. Fuselage effect on the windward side, formula (4)

As on the lee-side, the effect increases with $f_{M\left(\frac{A_H}{2}\right)}$

5. Dihedral of the main wing, formula (6)

The effect increases with $f_{M\left(\frac{A_H}{2}\right)}$

6. Body effect on main wing, formula (7)

Since it is due to equal changes of the angle of incidence at the tailplane as for low Mach numbers, it increases with $f_{M\left(\frac{A_H}{2}\right)}$

7. Plan form effect of the tailplane, formula (8)

Since C_{L_H} reasonably has to be taken including Mach number effects, the corresponding angle of incidence is smaller by $\frac{1}{f_{M(A_H)}}$. But all effects on each half tailplane for the same angle of attack increase with $f_{M\left(\frac{A_H}{2}\right)}$, so that altogether the effect has to be multiplied by

$$\frac{f_{M\left(\frac{A_H}{2}\right)}}{f_{M(A_H)}}$$

8. Plan form effect of the main wing, formula (9)

Considerations like those for the plan form effect at the tailplane give that $\left(\frac{\varepsilon_{vp}}{C_L}\right)_W C_L$ must be multiplied by

$$\frac{f_{M\left(\frac{A}{2}\right)}}{f_{M(A)}}$$

Both the lift slopes give two more factors, so that the total factor is

$$\frac{f_{M\left(\frac{A_H}{2}\right)}}{f_{M\left(\frac{A}{2}\right)}} \times \frac{f_{M\left(\frac{A}{2}\right)}}{f_{M(A)}} = \frac{f_{M\left(\frac{A_H}{2}\right)}}{f_{M(A)}}$$

9. Sweep-back of the tailplane, formula (10)

C_{L_H} is obtained with an angle of incidence decreased by $\frac{1}{f_{M(A_H)}}$. But our numerical factor includes considerations of this angle of attack, and it therefore must be increased by $f_{M\left(\frac{A_H}{2}\right)}$. The total factor is therefore

$$\frac{f_{M\left(\frac{A_H}{2}\right)}}{f_{M(A_H)}}$$

10. Sweep-back of the main wing, formula (11)

Analagous reasoning as in 9 gives a factor

$$\frac{f_{M\left(\frac{A}{2}\right)}}{f_{M(A)}}$$

which must be multiplied by $$\frac{f_{M\left(\frac{A_H}{2}\right)}}{f_{M\left(\frac{A}{2}\right)}}$$

so that the total factor is $$\frac{f_{M\left(\frac{A_H}{2}\right)}}{f_{M(A)}}$$

Additional assumptions have been that: 1. the downwash does not change with Mach number. 2. The correction factor for the aspect ratio, $G_{(A)}$, does not change with the Mach number.

If we consider first the effects independent of C_L or C_{L_H}, we find that they all are multiplied by the same factor $f_{M\left(\frac{A_H}{2}\right)}$. At a Mach number of $M = 0.8$ and for an aspect ratio of the tailplane $A_H = 4$, this factor has a value of 1.25. This may be regarded as a reasonable upper limit.

Those contributions depending on C_L and C_{L_H} decrease with Mach number. The contributions 8 and 10 are usually small compared with those of 7 and 9. Both, 7 and 9, have the factor

$$\frac{f_{M\left(\frac{A_H}{2}\right)}}{f_{M(A_H)}}$$

At a Mach number $M = 0.8$, and for a tailplane aspect ratio of even $A_H = 6$, the factor has a value of 0.92. Thus the decrease is unlikely to be more than 8% which we may neglect.

As a rough rule, we can therefore include the effect of Mach numbers up to 0.8 by multiplying only those contributions to the rolling moment coefficient which are independent of C_L or C_{L_H} by the factor

$$f_{M\left(\frac{A_H}{2}\right)} = \frac{1 + \frac{4}{A_H}}{\sqrt{1 - M^2} + \frac{4}{A_H}} \qquad (15)$$

TABLE I

Comparison of calculated and experimental values of rolling-moment coefficients K per radian angle of sideslip

Aircraft	Typhoon	Hastings	Spitfire	Spearfish	Brabazon	Firefly	Wywern II	Aircraft Ref.10
End plate effect	0.0192	0.0992	0.0403	0.0447	0.1160	+0.0199	+0.0967	0.0484
Dihedral of tailplane	0	0	0	0	0	0	-0.0924	0
Fuselage-effect, Lee-side	-0.0798	-0.0611	-0.0922	-0.0640	-0.0501	-0.1006	-0.0576	-0.0801
Fuselage-effect, Wind-side	-0.0270	0	-0.0274	-0.0303	0* *due to long dorsal fin	-0.0495	-0.0155	-0.0302
Dihedral of wing	0.0100	0.0047	0.0111	0.0079	0.0055	+0.0107	+0.0076	0.0121
Fuselage-effect to wing	-0.0365	-0.0313	-0.0252	0	-0.0121	-0.0416	-0.0380	-0.0397
Estimated without tolerances: Lee-side	-0.0835	-0.0248	-0.0791	-0.0377	+0.0046	-0.1061	-0.0705	-0.0697
Estimated without tolerances: Wind-side	-0.0306	+0.0363	-0.0143	-0.0040	+0.0547	-0.0550	-0.0287	-0.0198
Estimated without tolerances: Total	-0.1141	+0.0115	-0.0934	-0.0417	+0.0593	-0.1611	-0.0091	-0.0895
Tolerances	±0.025	±0.025	±0.025	±0.025	±0.025	±0.025	±0.025	±0.025
Estimated	-0.089 -0.139	+0.037 -0.013	-0.068 -0.118	-0.017 -0.067	+0.084 +0.034	-0.136 -0.186	-0.074 -0.124	-0.064 -0.114
Measured	-0.115	+0.034	-0.115	-0.029	+0.077	-0.155	-0.120	-0.086

TABLE II

Detailed results of some measurements

TYPHOON

K	Propeller	Wing incidence	Sideslip
-0.121	without propeller	5.7°	β=10°, right wing forward
-0.110	" "	-0.65°	" " " "
-0.119	with propeller, no thrust	5.7°	" " " "
-0.090	" " " "	-0.65°	" " " "
-0.124	" " " "	5.7°	β=-10°, left wing forward
-0.121	" " " "	-0.65°	" " " "
-0.133	with propeller and thrust	5.7°	β=10°, right wing forward
-0.084	" " " "	-0.65°	" " " "
-0.133	" " " "	5.7°	β=-10°, left wing forward
-0.107	" " " "	-0.65°	" " " "

Average: -0.115

BRABAZON

K	Propeller	Elevator Deflect.	Tailplane-Setting	Sideslip
0.084	without propeller	η = 0°	ε = 2° 50'	β = 10°
0.091	" "	"	"	15°
0.069	" "	"	ε = 0° 50'	10°
0.085	" "	"	"	15°
0.078	" "	η = 10°	ε = 2° 50'	10°
0.093	" "	"	"	15°
0.065	" "	"	ε = 0° 50"	10°
0.071	" "	"	"	15°
0.064	" "	η = -10°	"	10°
0.070	" "	"	"	15°

Average: 0.077

NACA-FLIGHT MEASUREMENT, REF.10

K	Power	Lift	Sideslip
-0.081	off	C_L = 0.8	β=10°, right wing forward
-0.087	"	C_L = 0.2	" " " "
-0.065	"	C_L = 0.8	β=-10°, left wing forward
-0.062	"	C_L = 0.2	" " " "
-0.080	on	C_L = 0.8	β=10°, right wing forward
-0.093	"	C_L = 0.2	" " " "
-0.114	"	C_L = 0.8	β=-10°, left wing forward
-0.110	"	C_L = 0.2	" " " "

Average: -0.086

FIREFLY

K	Wing incidence	Elevator Deflect.	Sideslip	Kind of measurem.
-0.218	α = 0	η = 3.5°	β = 2°	force
-0.139	"	"	"	pressure distrib.
-0.155	α = 0.2°	η = 3°.	β = 5°	force
-0.110	"	"	"	pressure distrib.

Average: -0.155

Wt.2078.CP.119.K3. Printed in Great Britain.

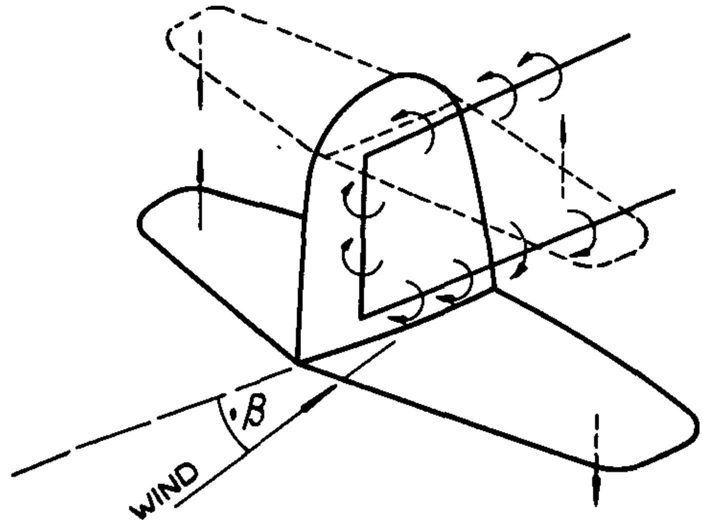

FIG. 1. SKETCH SHOWING THE VORTICES WHICH INDUCE THE ROLLING-MOMENT DUE TO THE LIFT ON THE FIN & RUDDER.

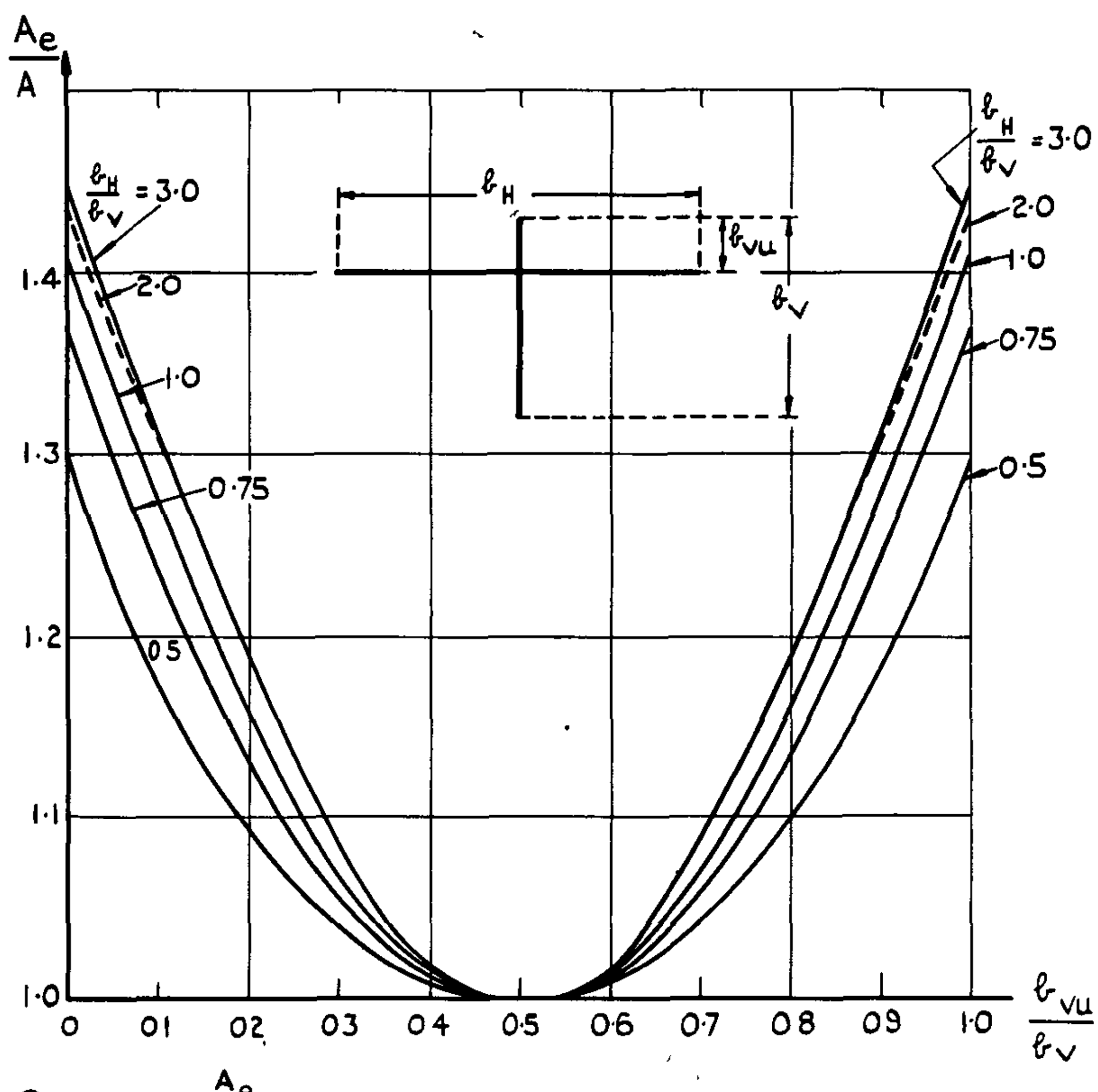

FIG. 2. FACTOR $\frac{A_e}{A}$, BY WHICH THE GEOMETRIC ASPECT-RATIO OF THE FIN & RUDDER HAS TO BE MULTIPLIED TO ALLOW FOR THE END-PLATE EFFECT OF THE TAILPLANE. THEORETICAL VALUES, CORRECTED ACCORDING TO MEASUREMENTS.

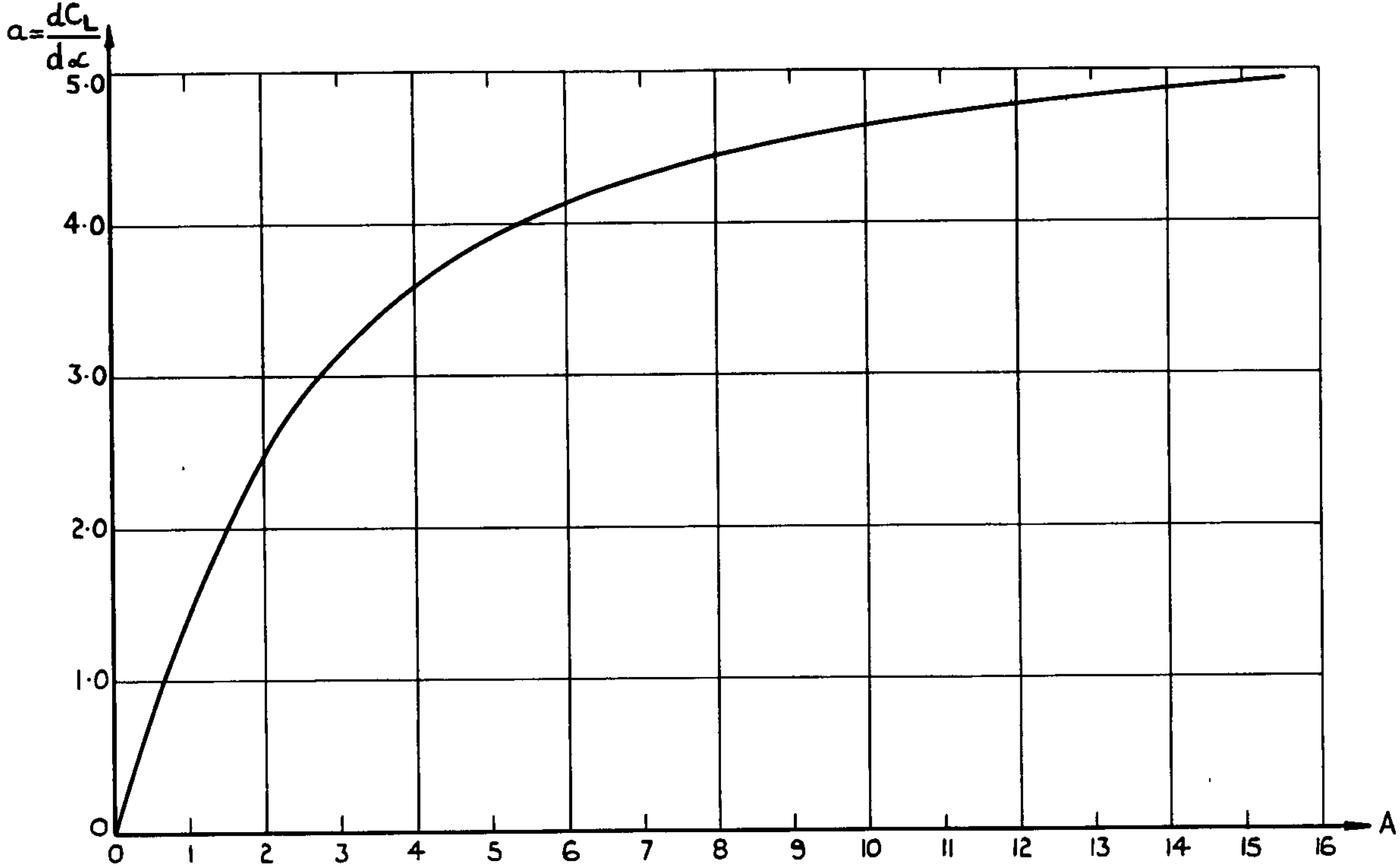

FIG. 3. LIFT CURVE SLOPE AGAINST ASPECT-RATIO.
LIFTING SURFACE THEORY WITH $a_\infty = 2\pi \times 0{\cdot}88$.

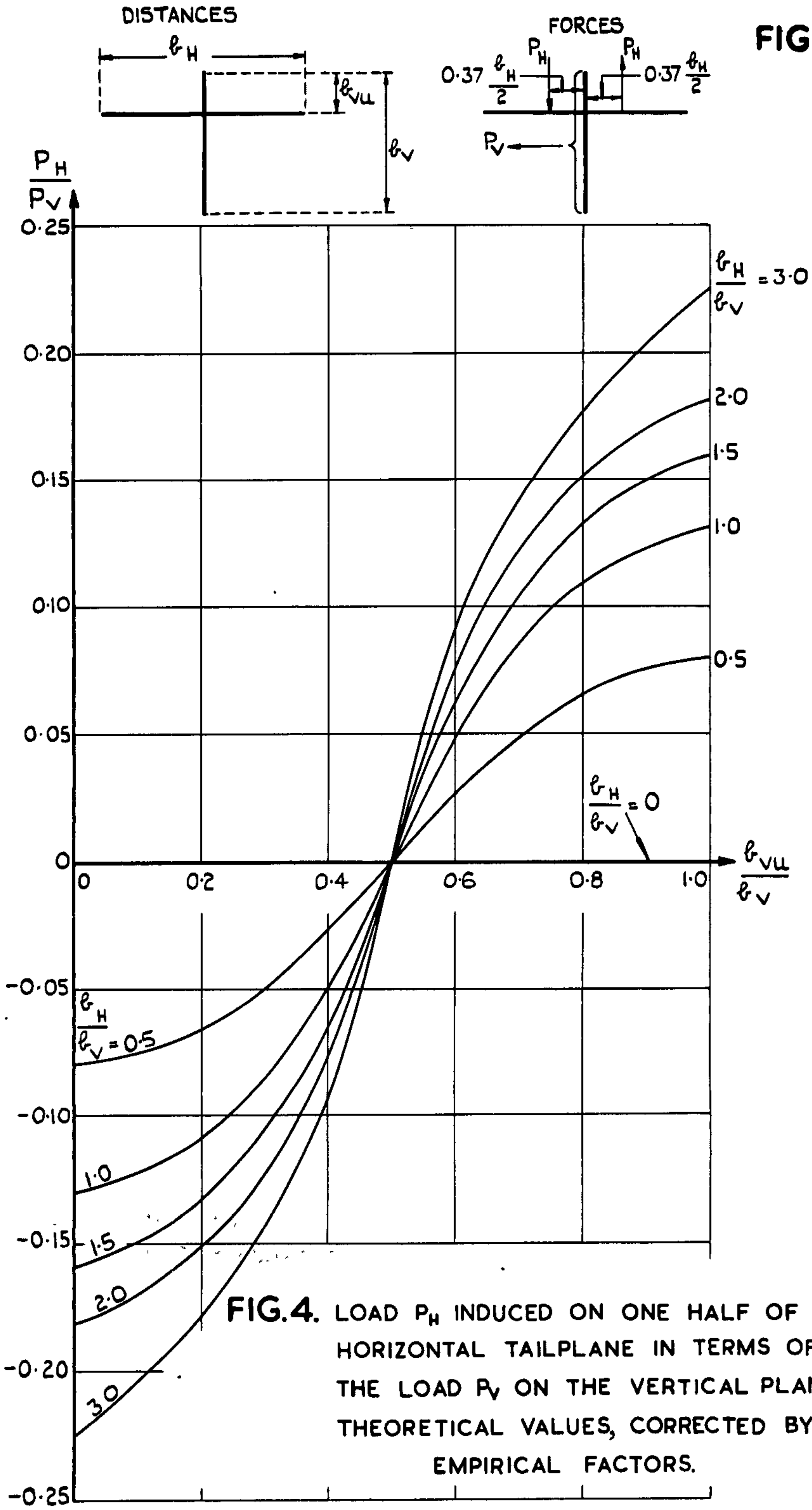

FIG. 4. LOAD P_H INDUCED ON ONE HALF OF THE HORIZONTAL TAILPLANE IN TERMS OF THE LOAD P_V ON THE VERTICAL PLANE. THEORETICAL VALUES, CORRECTED BY EMPIRICAL FACTORS.

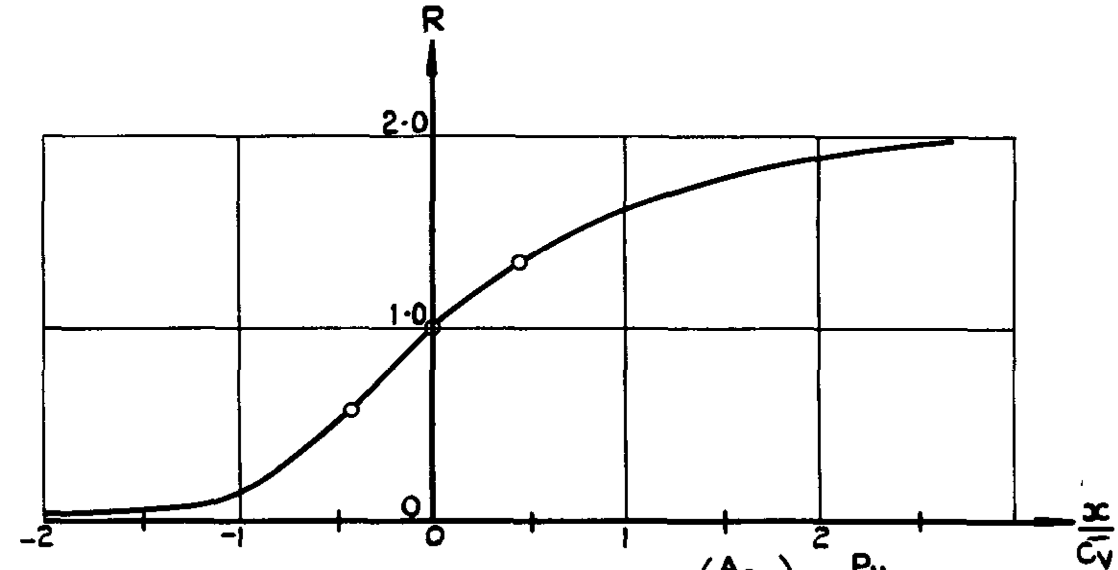

FIG. 5. FACTOR R FOR CORRECTION OF $\left(\frac{A_e}{A}-1\right)$ & $\frac{P_H}{P_V}$ TO CONSIDER THE HORIZONTAL POSITION OF THE TAILPLANE RELATIVE TO FIN & RUDDER. x = POSITION OF THE ¼-CHORD LINE OF THE TAILPLANE BEHIND THE ¼-CHORD LINE OF THE FIN & RUDDER $\bar{c}_V$.

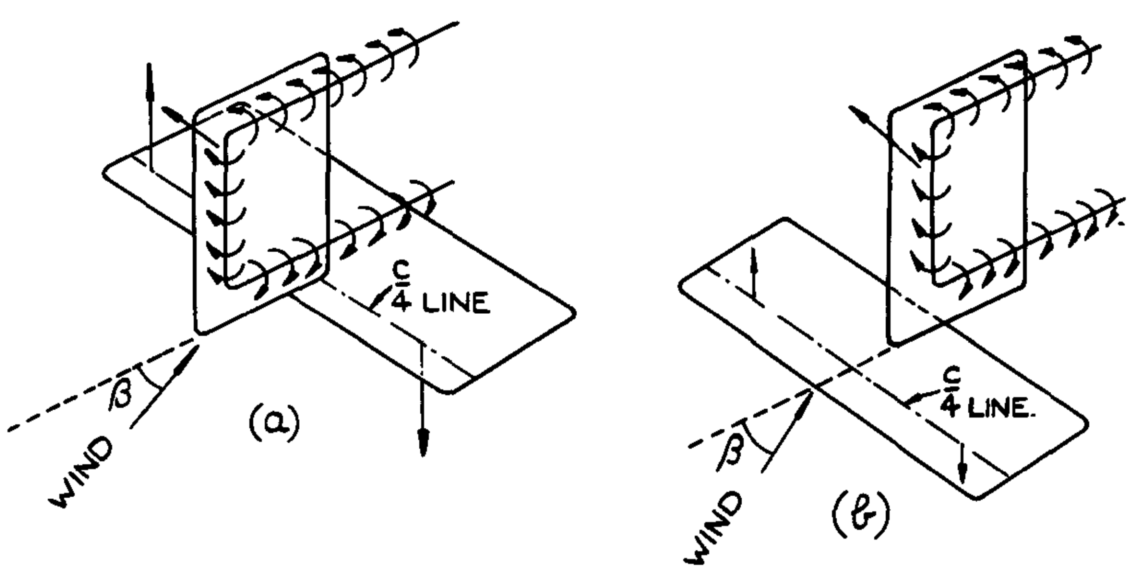

FIG. 6. SKETCH OF THE VORTICES OF THE FIN SHOWING THE DIFFERENT INFLUENCES ON A TAILPLANE IN REARWARD (a) AND FORWARD (b) HORIZONTAL POSITIONS.

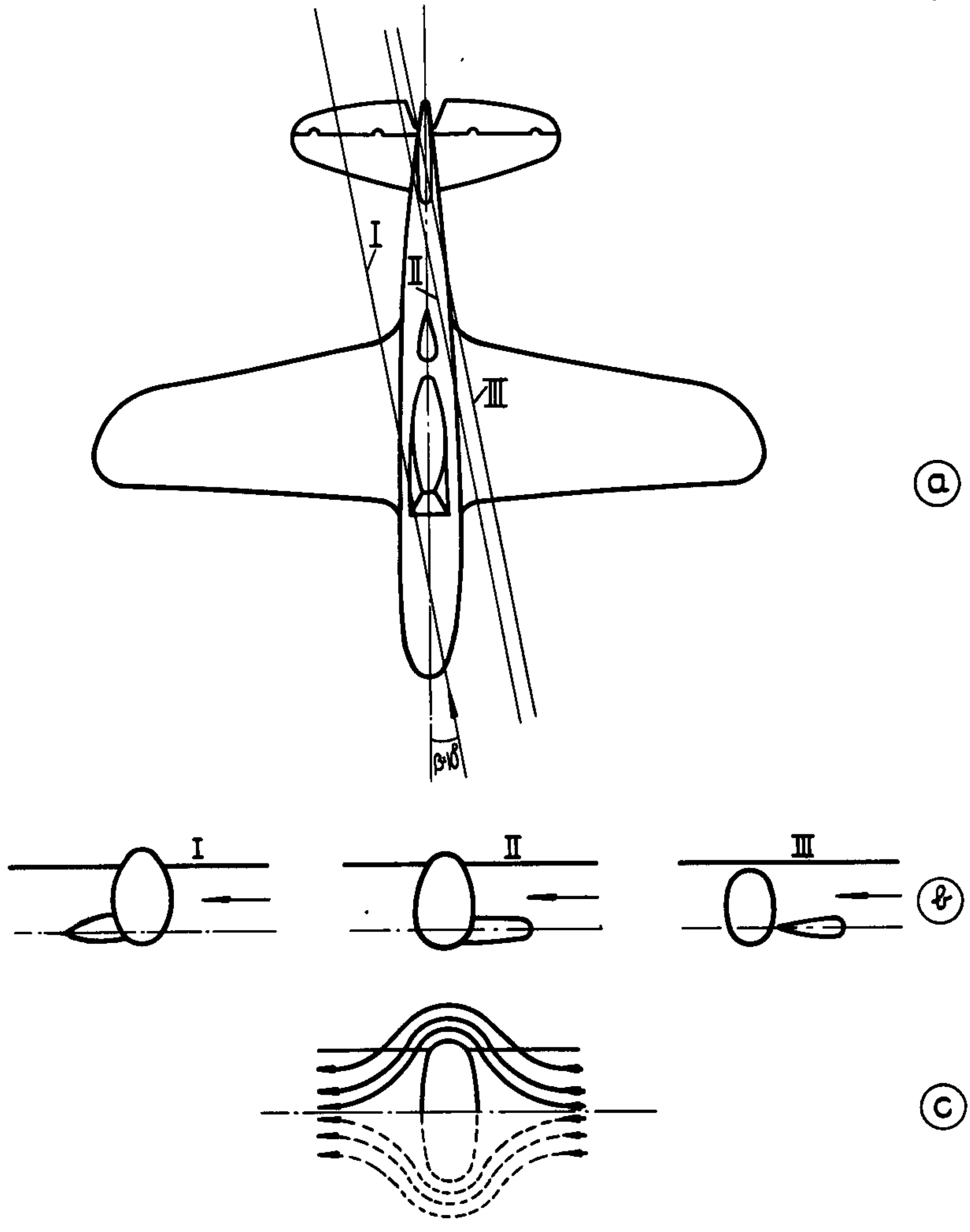

FIG. 7. SKETCH EXPLAINING THE ASSUMPTIONS FOR CALCULATING THE FUSELAGE-INFLUENCE ON THE LEE-SIDE.

(a) STREAMLINES PASSING AN AIRCRAFT AT 10° SIDESLIP (AIRCRAFT OF REF 10)

(b) BODY SECTIONS WHICH ARE CROSSED BY THE STREAMLINES I, II & III IF THE VELOCITY IS SPLIT IN A COMPONENT PARALLEL TO THE AIRCRAFT CENTRE LINE, & ANOTHER PERPENDICULAR TO THIS

(c) PATTERN WHICH SHOULD REPLACE THE LATERAL FLOW AT ALL SECTIONS

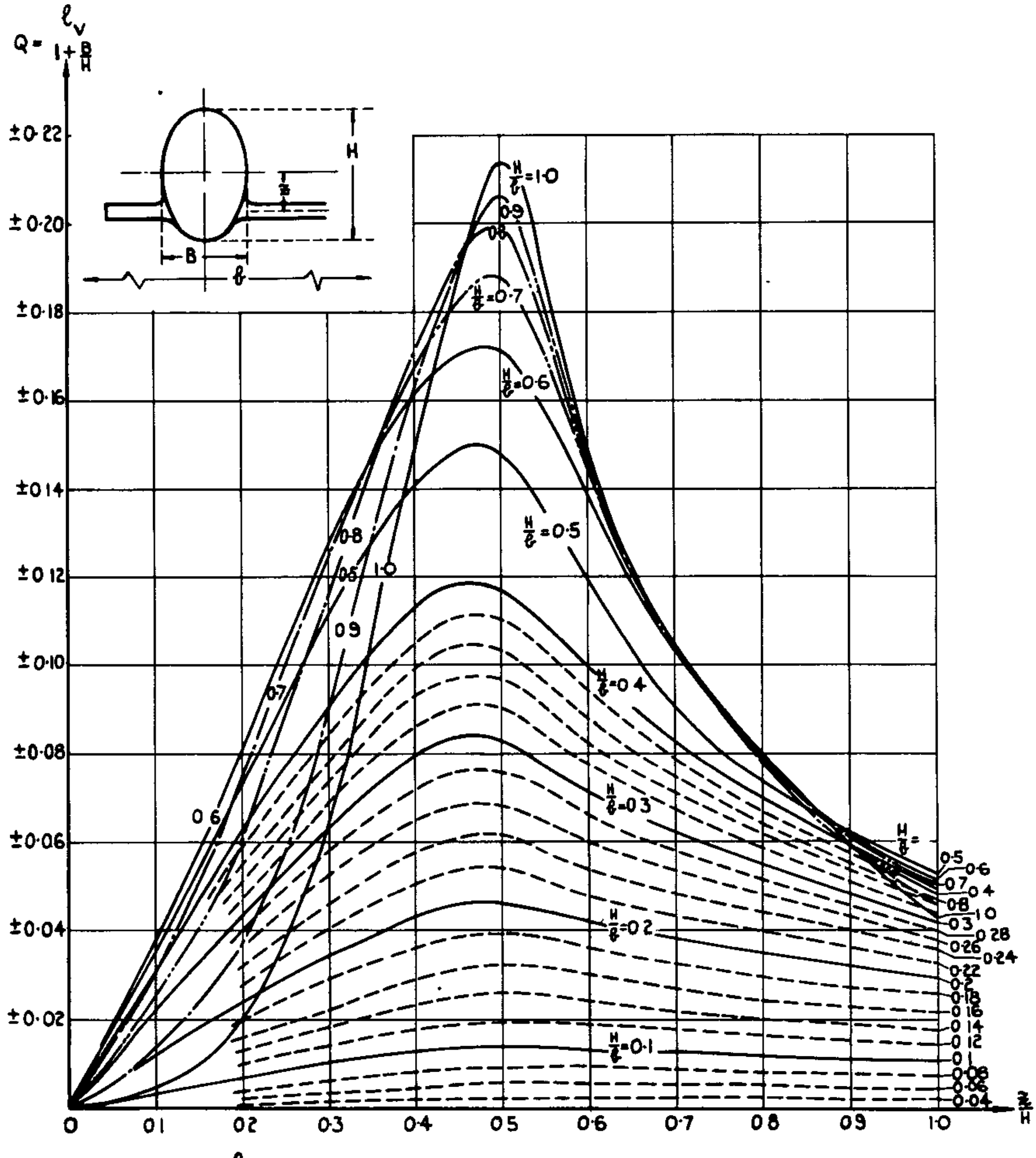

FIG. 8. $Q = \frac{\ell_v}{1+\frac{B}{H}}$ PER RADIAN SIDESLIP, GIVING THE ROLLING MOMENT DUE TO FUSELAGE EFFECT FOR ELLIPTICAL WINGS OF ASPECT-RATIO A=6.

Q IS POSITIVE FOR LOW-WING ARRANGEMENTS, NEGATIVE FOR HIGH-WINGS.

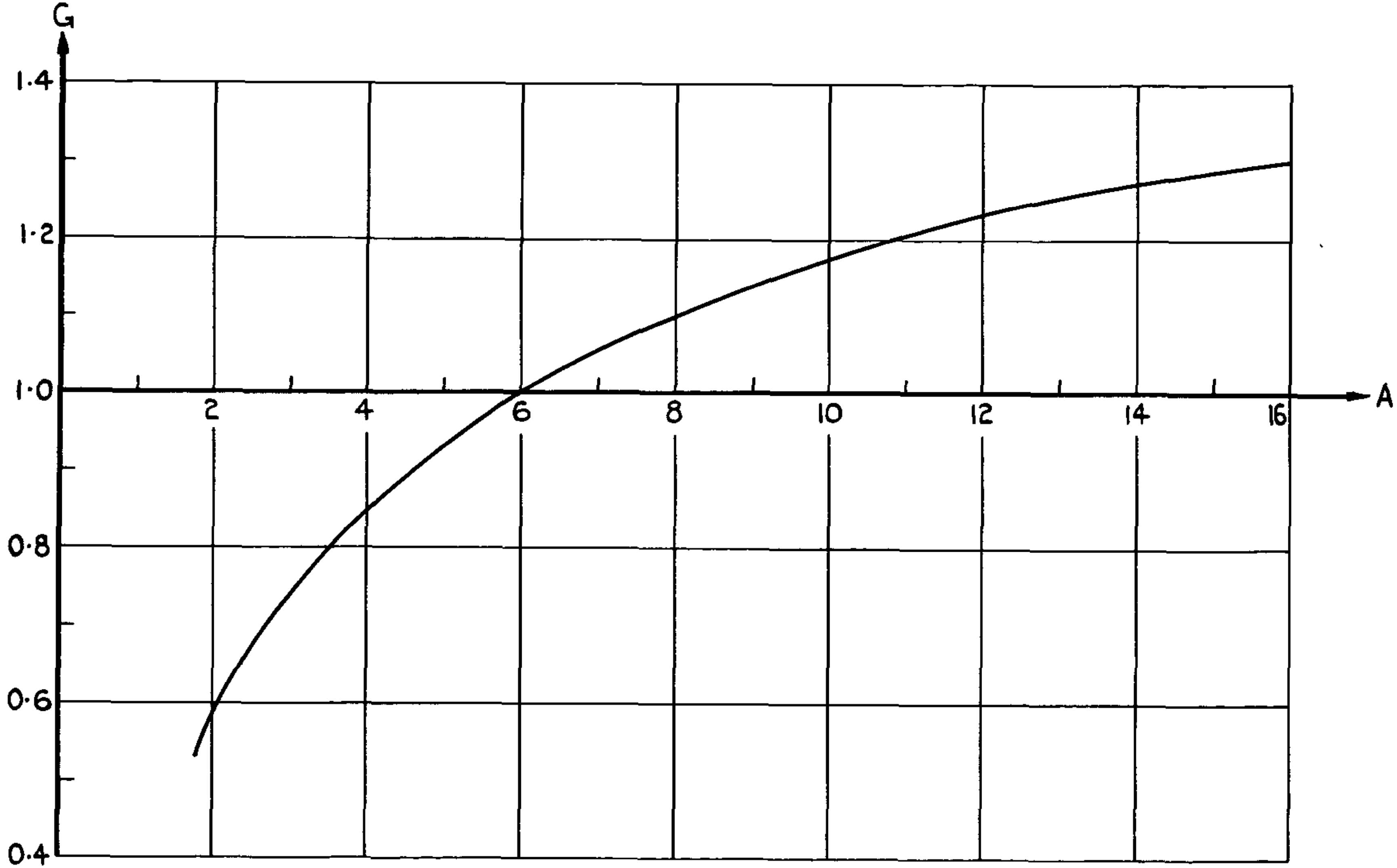

FIG. 9. FACTOR G, WHICH ALLOWS FOR ASPECT RATIOS DIFFERING FROM A = 6.

FIG. 9

FIG. 10(a)

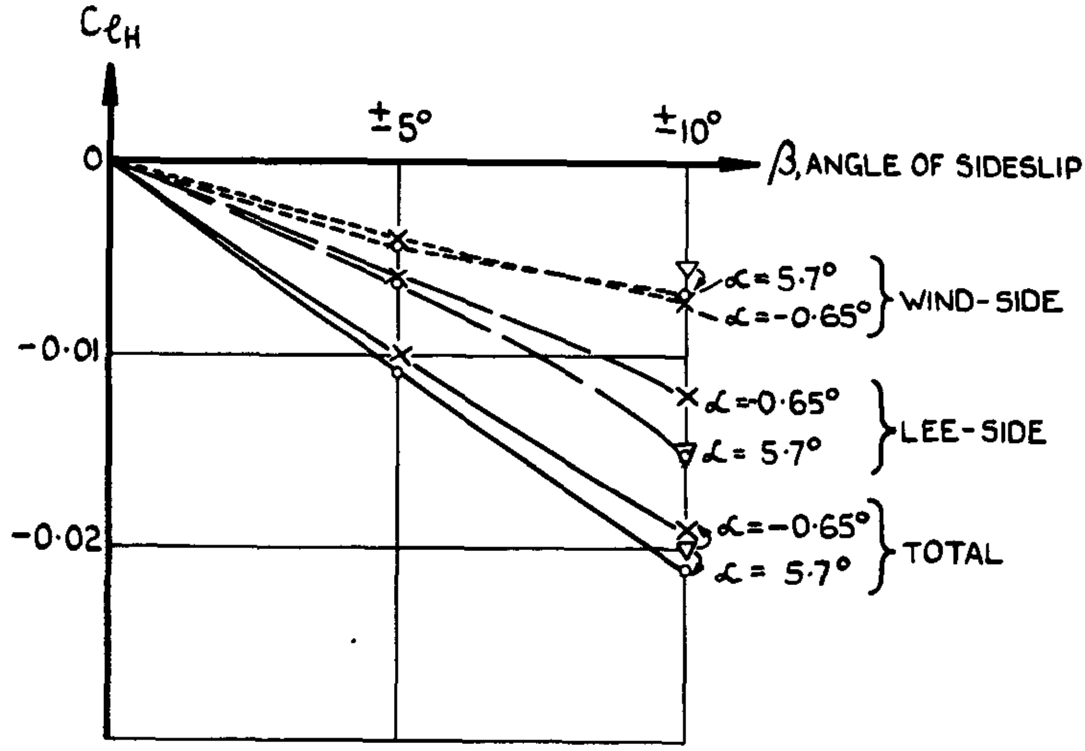

FIG. 10 (a) TYPHOON MODEL MEASUREMENT, WITHOUT PROPELLER (REF. 9).

TAILPLANE ROLLING MOMENT C_{l_H} AGAINST ANGLE OF SIDESLIP, C_{l_H} POSITIVE, IF IT TENDS TO TURN DOWN THE WINDWARD SIDE. ∇ = CALCULATED

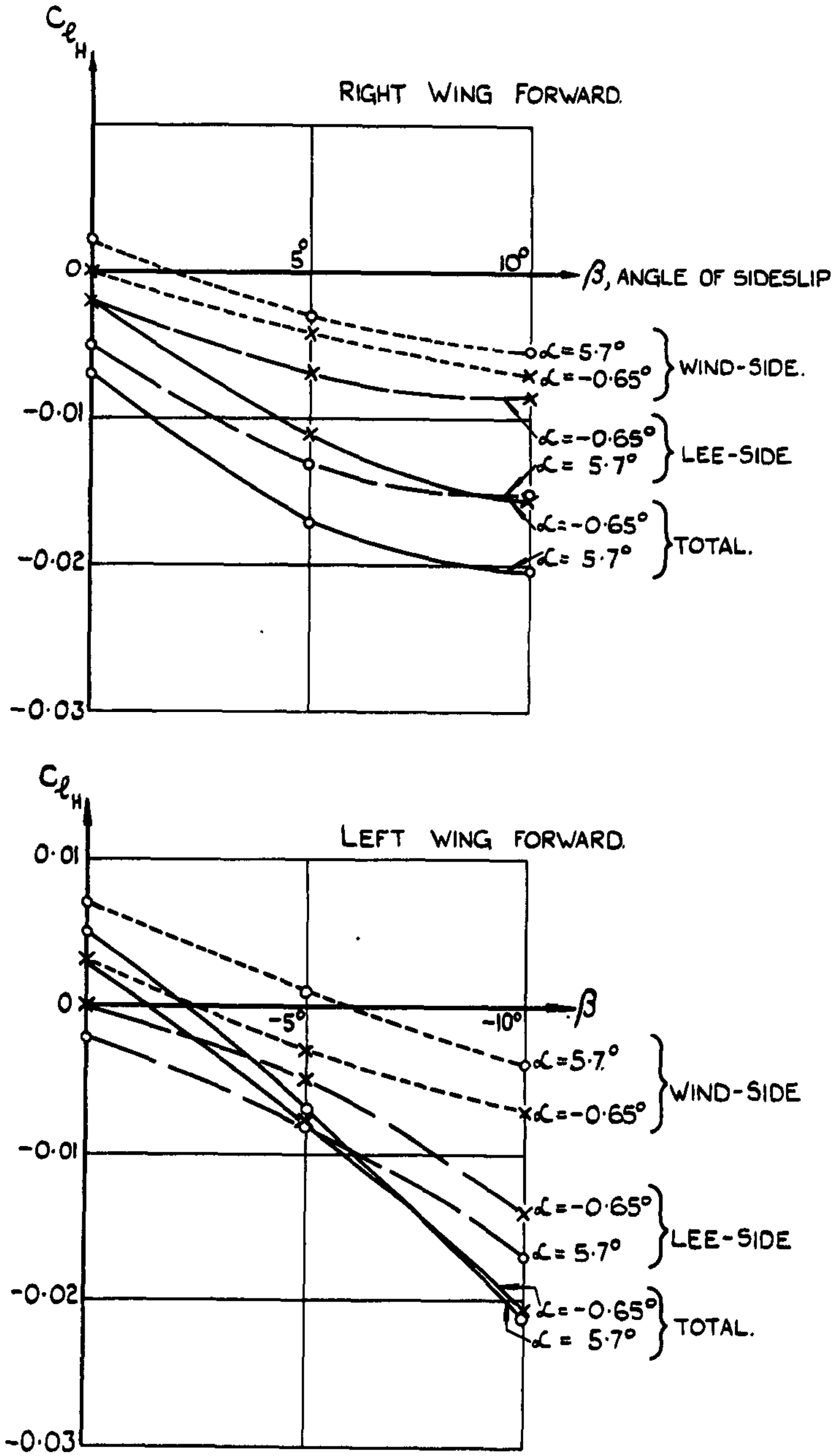

FIG. 10 (b) TYPHOON MODEL MEASUREMENT. WITH PROPELLER, NO THRUST, $T_c = 0$.

TAILPLANE ROLLING MOMENT C_{l_H} AGAINST ANGLE OF SIDESLIP.
C_{l_H} POSITIVE, IF IT TENDS TO TURN DOWN THE WINDWARD SIDE.

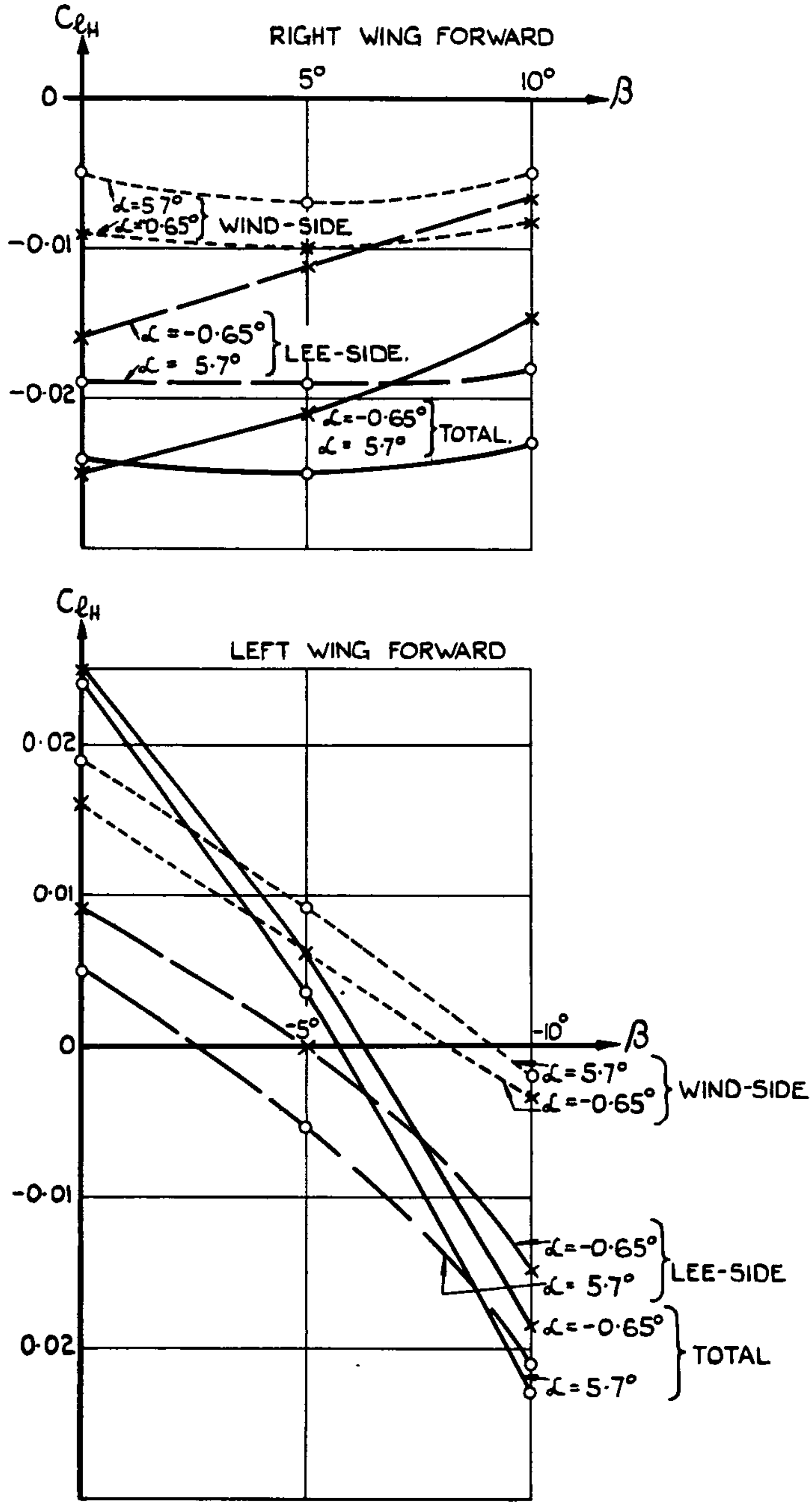

FIG.10(c) TYPHOON MODEL MEASUREMENT.
WITH PROPELLER, THRUST T_C=0·04.
TAILPLANE ROLLING MOMENT C_{l_H} AGAINST ANGLE OF SIDESLIP

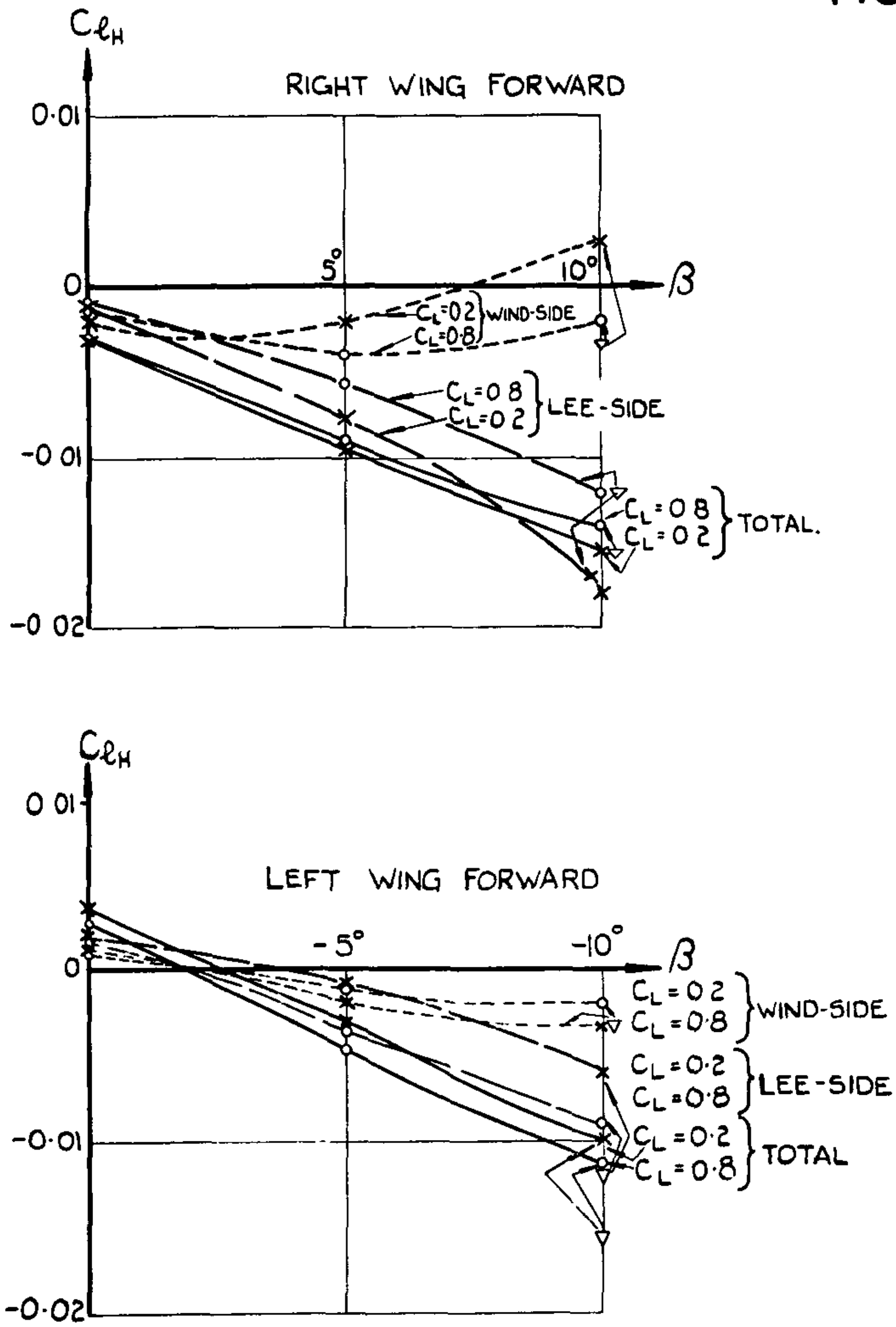

FIG. 11(a) NACA FLIGHT-MEASUREMENTS OF REF. 10. POWER OFF.

TAILPLANE ROLLING MOMENT C_{ℓ_H} AGAINST ANGLE OF SIDESLIP.
C_{ℓ_H} POSITIVE IF IT TENDS TO TURN DOWN WINDWARD SIDE.
∇ = CALCULATED WITHOUT PROPELLER.

THE REFERRED ROLLING MOMENT AT β =0 WITHOUT ASYMMETRICAL LOADS IS TAKEN AS AVERAGE OF THE FOUR APPROPRIATE MEASUREMENTS RIGHT SIDE, LEFT SIDE, EACH WITH POWER OFF AND ON

FIG. 11(b)

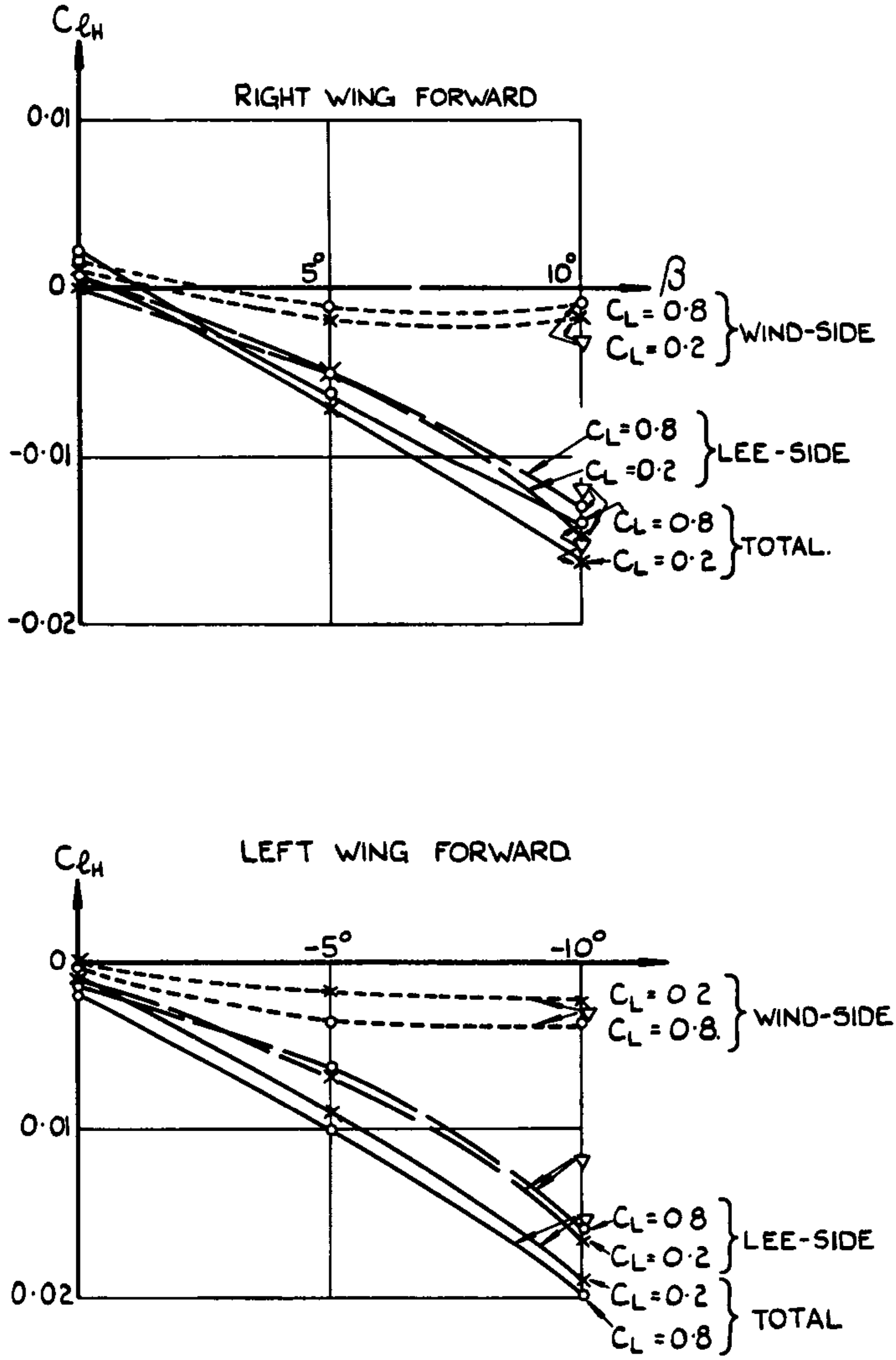

FIG. 11(b). N A C A FLIGHT-MEASUREMENTS OF REF. 10. POWER ON.

TAILPLANE ROLLING MOMENT C_{ℓ_H} AGAINST ANGLE OF SIDESLIP
▽ = CALCULATED WITHOUT PROPELLER.

FIG.12.

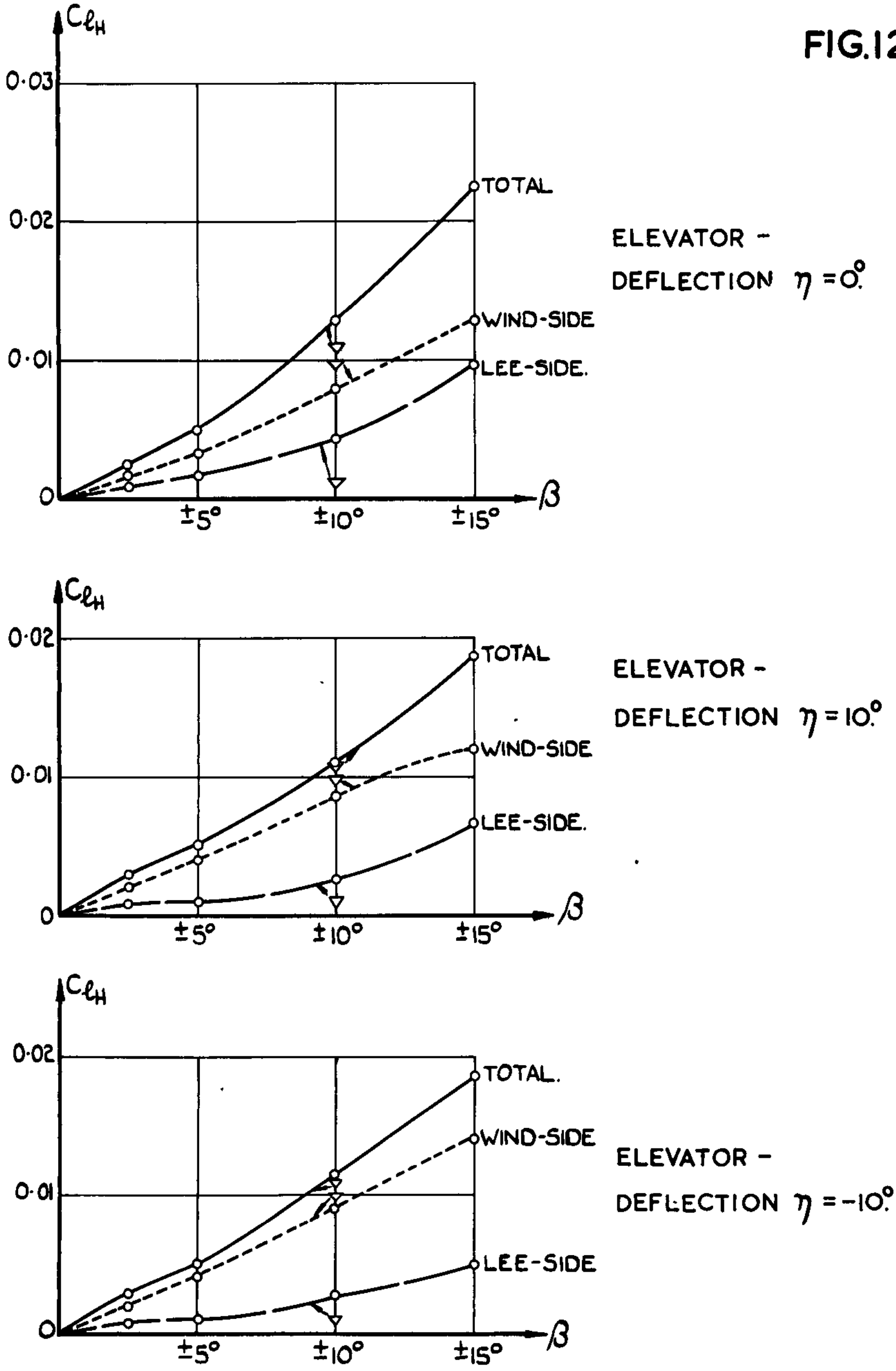

FIG.12. BRABAZON WIND-TUNNEL MEASUREMENTS, TAIL-PLANE SETTING ε = 50′ (REF. 11.)

TAILPLANE ROLLING-MOMENT C_{ℓ_H} AGAINST ANGLE OF SIDESLIP.
C_{ℓ_H} POSITIVE IF IT TENDS TO TURN DOWN THE WINDWARD SIDE.
∇ = CALCULATED.

FIG.13.

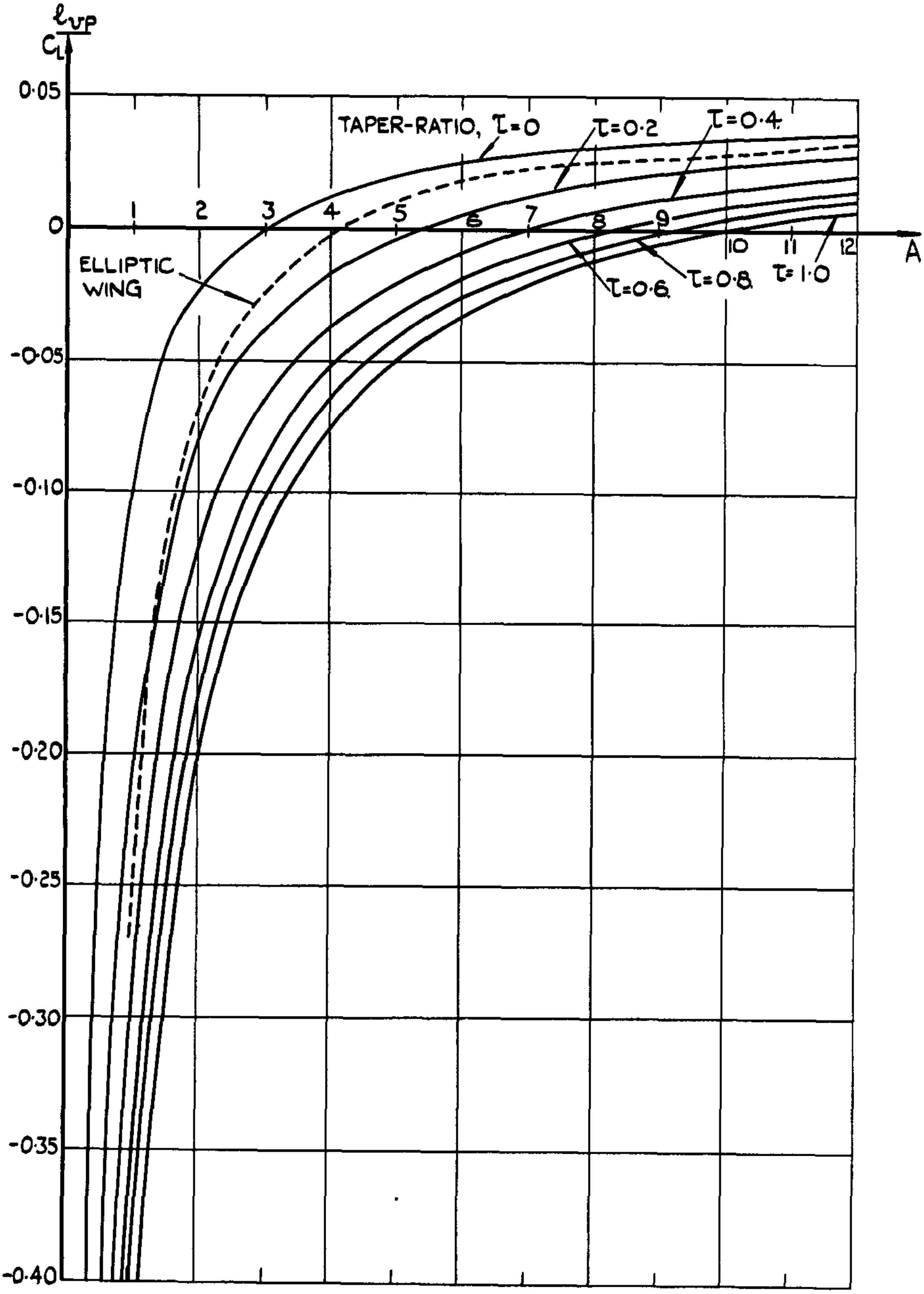

FIG.13. EFFECT OF THE WING PLAN FORM.

ROLLING-MOMENT COEFFICIENT PER RADIAN ANGLE OF SIDESLIP, DIVIDED BY C_L, FOR VARIOUS ASPECT-RATIOS & WING PLAN FORMS.

FIG. 14.

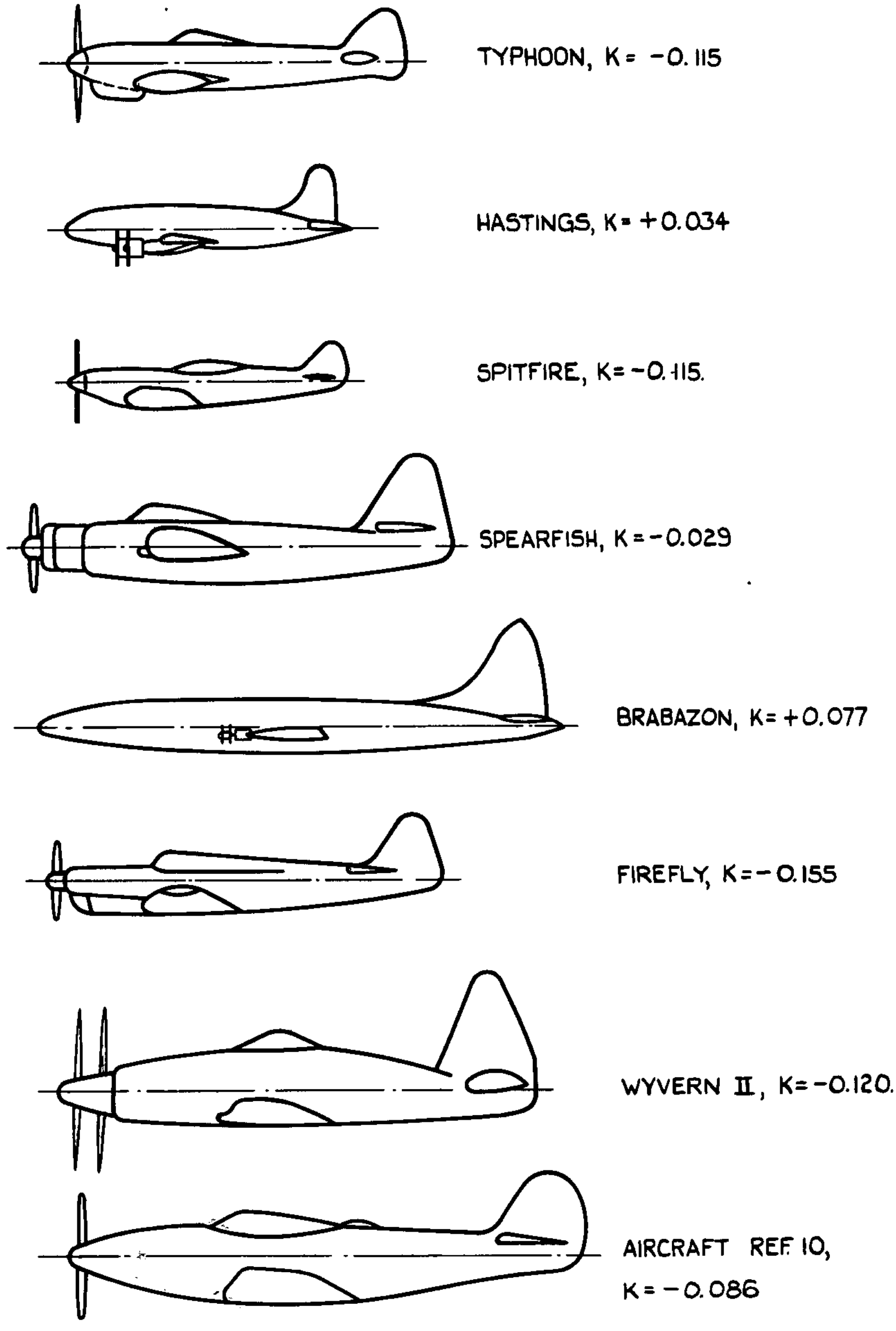

FIG. 14. SIDE-VIEWS OF AIRCRAFT CONSIDERED IN TABLE I.

(WITH MEASURED VALUES OF K.)

FIG.15.

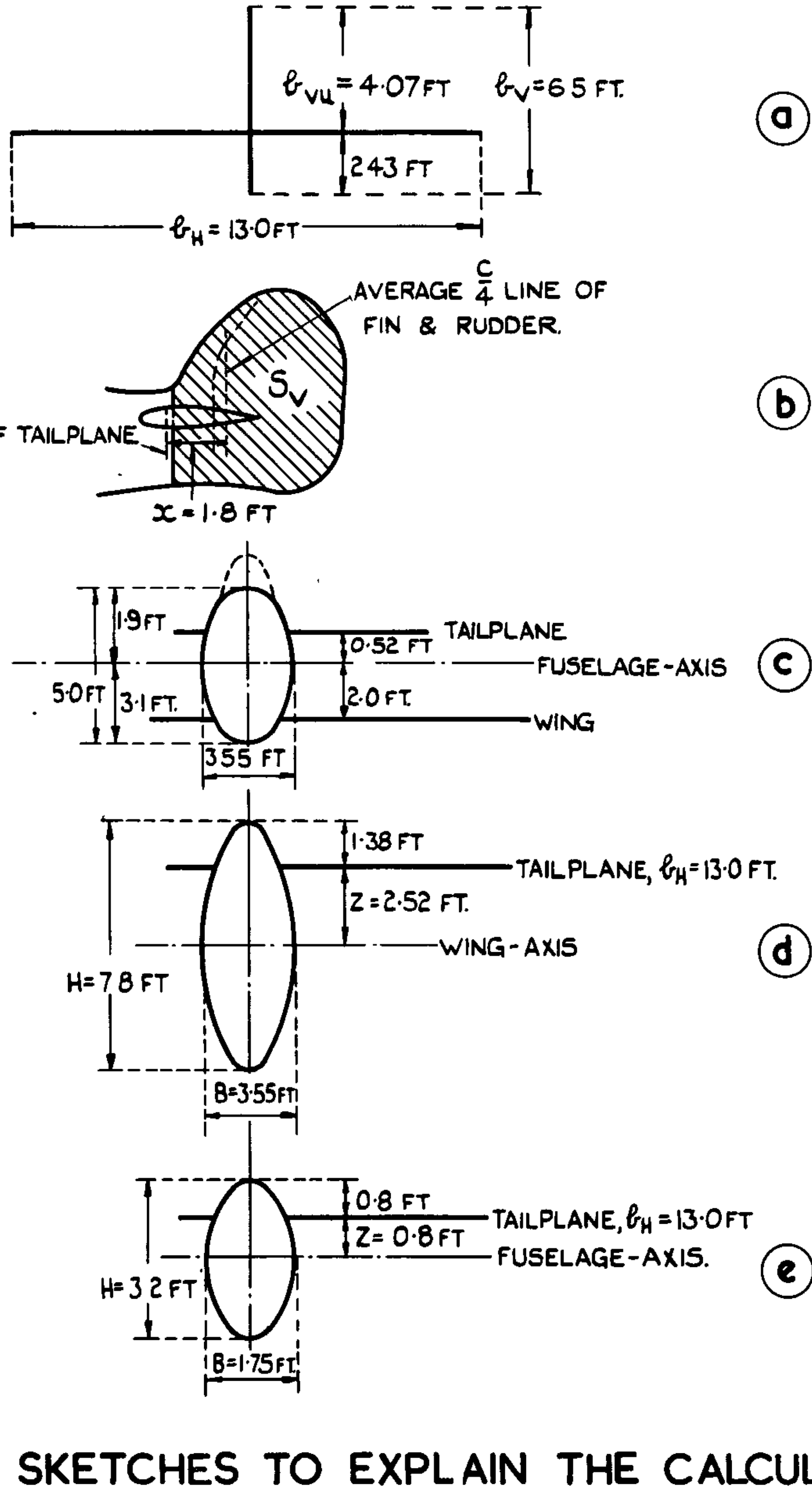

FIG.15. SKETCHES TO EXPLAIN THE CALCULATION FOR THE TYPHOON.

a, CROSS-SECTION AT THE TAIL.
b, SIDE-VIEW OF THE FIN & RUDDER SHOWING THE DISTANCE x
c, CROSS-SECTION AT THE MAIN WING WITH THE POSITION OF THE TAILPLANE TO THIS SECTION.
d, CROSS-SECTION DERIVED FROM (c) USED FOR REPLACING THE LATERAL FLOW.
e, CROSS-SECTION AT THE LEADING-EDGE OF THE TAILPLANE.

C.P. No. 119
(14,969)
A.R.C. Technical Report

PUBLISHED BY HER MAJESTY'S STATIONERY OFFICE

To be purchased from

York House, Kingsway, LONDON, W.C.2. 423 Oxford Street, LONDON, W 1

P.O Box 569, LONDON, S.E.1

13a Castle Street, EDINBURGH, 2 | 1 St Andrew's Crescent, CARDIFF

39 King Street, MANCHESTER, 2 | Tower Lane, BRISTOL, 1

2 Edmund Street, BIRMINGHAM, 3 | 80 Chichester Street, BELFAST

or from any Bookseller

1953

Price 8s. 6d. net

PRINTED IN GREAT BRITAIN

S.O. Code No. 23-9007-19